Solvent and Vibrational Effects on Nonlinear Optical Properties

Peter Macák

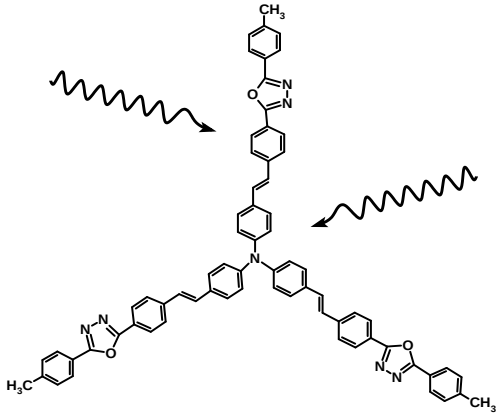

Royal Institute of Technology
Stockholm, 2002

ISBN-91-7283-267-3
Stockholm 2002

Abstract

This work presents analyses, development and applications of theoretical models for studies of solvent and vibrational effects on nonlinear optical properties of molecules. Response theory *ab initio* quantum chemistry methods are applied to large organic molecules.

Current dielectric continuum reaction field models for solvent effects on nonlinear optical properties are analyzed and categorized into two groups depending on the type of field used for the definition of the solute nonlinear optical properties. Analytical connections between the approaches are derived together with consistent local field factors. Traditional Lorentz-Lorenz local field factors are shown to be consistent with the local field factors based on reaction field models provided that a cavity field factor at the output frequency is included in the latter models. A semiclassical model is generalized for ellipsoidal shapes of cavities including vibrational contributions and is applied to conjugated polymers and fullerenes. A study on push-pull polyenes revealed, in contrast to previous studies on stilbene derivatives, that the two-photon absorption cross section has different behavior compared to the second hyperpolarizability with respect to the solvent polarity and that it displays saturation.

Vibrational effects on two-photon absorption are studied within a Herzberg-Teller approach. The surprisingly large enhancement of the two-photon absorption cross section in multi-branched molecules observed experimentally is shown to be essentially due to vibronic coupling. A method for calculating the spectral profile of vibrationally induced two-photon absorption using the linear coupling model is presented together with sum rules for vibrationally induced two-photon absorption.

Structure-to-property relations are studied for two-photon absorption cross sections in one dimensional donor/acceptor substituted π-conjugated molecules. It is found that, while the molecular length and the one-photon absorption intensity are quite strongly correlated factors, the corresponding correlation for the two-photon absorption is much weaker or is missing. In contrast, the most crucial role for large two-photon absorption is played by the π center. The chromophore based on dithienothiophene as π center attached with symmetrical N,N-diphenylamine donors is found to have the largest two-photon absorption cross section in the visible region among all the studied one-dimensional organic materials.

A dynamical density matrix based theory of two-photon absorption (TPA) is presented. The importance of the role of pulse duration, dephasing and resonant conditions on the final TPA cross section are analysed. A breakdown of the conventional identification of the coherent one-step process is predicted for long pulse duration where the incoherent two-step process is found to be dominating. The major role of the solvent is to enhance the off-resonant contributions to the TPA due to the short collisional dephasing time compared to the lifetime of the excited states involved. Together with *ab initio* calculations the presented theory provides agreement with experimental data for recently measured charge-transfer molecules.

Keywords

Nonlinear optics, solvent effects, vibrational effects, local field factors, two-photon absorption, reaction field.

List of papers included in the thesis

Paper I. P. Norman, P. Macak, Y. Luo and H. Ågren, **Vibrational contributions to solute molecular properties obtained through a semiclassical model employing ellipsoidal cavities.** *J. Chem. Phys.*, **110**, 7960-7965 (1999).

Paper II. Y. Luo, P. Norman, P. Macak and H. Ågren, **Solvent effects on the polarizabilities and hyperpolarizabilities of conjugated polymers.** *J. Chem. Phys.*, **111**, 9853-9858 (1999).

Paper III. P. Macak, P. Norman, Y. Luo and H. Ågren, **Modeling of dynamic molecular solvent properties using local and cavity field approaches.** *J. Chem. Phys.*, **112**, 1868-1875 (2000).

Paper IV. Y. Luo, P. Norman, P. Macak and H. Ågren, **Nonlinear optical susceptibilities of fullerenes in the condensed phase.** *Phys. Rev. B*, **61**, 3060-3066 (2000).

Paper V. Y. Luo, P. Norman, P. Macak and H. Ågren, **Solvent-induced two-photon absorption of a push-pull molecule.** *J. Phys. Chem. A*, **104**, 4718-4722 (2000).

Paper VI. P. Macak, Y. Luo, P. Norman and H. Ågren, **Electronic and vibronic contributions to two-photon absorption of molecules with multi-branched structures.** *J. Chem. Phys. 113*, **17**, 7055-7061 (2000).

Paper VII. P. Macak, Y. Luo and H. Ågren, **Simulations of vibronic profiles in two-photon absorption.** *Chem. Phys. Lett.*, **330**, 447-456 (2000).

Paper VIII. R. W. Munn, Y. Luo, P. Macak and H. Ågren, **Role of the cavity field in non-linear optical response in the condensed phase.** *J. Chem. Phys.*, **114**, 3105-3108 (2001).

Paper IX. C. K. Wang, P. Macak, Y. Luo and H. Ågren, **Effects of π-centers and symmetry on two-photon absorption cross sections of organic chromophores.** *J. Chem. Phys.* **114**, 9813-9820 (2001).

Paper X. F. Gel'mukhanov, A. Baev, P. Macak, Y. Luo and H. Ågren, **Dynamics of two-photon absorption by molecules and solutions.** *J. Opt. Soc. Am. B*, **19**, No. 5, 000, (2002).

Paper XI. A. Baev, F. Gel'mukhanov, P. Macak, H. Ågren and Y. Luo, **General theory for pulse propagation in two-photon active media.** Submitted to *J. Chem. Phys.*, (2002).

Paper XII. P. Macak, **Analytical evaluation of excited state energy gradients for large molecules.** In Preparation.

List of related papers not included in the thesis

Paper XIII. P. Macak, Y. Luo, P. Norman and H. Ågren, **Semi-classical modeling of medium effects on NLO molecular properties.** *Non-linear Optics*, **25**, 172-182 (2000).

Paper XIV. Y. Luo, P. Macak, P. Norman, C. K. Wang and H. Ågren, **Ab initio calculations of structure-to-property relations for two-photon absorption of organic molecules.** *Nonlinear Optics*, **27**, 33-46 (2001).

My contribution to papers in the thesis

- I made all the model and method development together with the calculations in **papers I, III, VI** and **VII**.
- I have contributed to the generalization of the semiclassical model to ellipsoidal shape cavities in **papers II** and **V**. I derived the formulas for the Onsager-Bötcher relation based approach in **paper IV**.
- I made the suggestion that the cavity field factor at the output frequency should indeed be included to the local field factors based on the cavity approach in **paper VIII**.
- I have applied the few state model and calculated necessary transition dipole moments for the interpretation of the calculations in **paper IX**.
- I carried out the *ab initio* calculations of the transition moments used in the density matrix formalism in **papers X, XI** and I have also participated in analyses of the problem and in the development of the dynamical model.
- I have performed all the work in the preparation of **paper XII**.

Contents

1 Introduction **1**

2 Nonlinear optical processes **5**
2.1 Macroscopic description 5
2.1.1 Electromagnetic fields 5
2.1.2 Susceptibilities 6
2.1.3 Non-resonant processes 7
2.1.4 Absorption processes 8
2.2 Microscopic description 9
2.2.1 Interaction of light with molecules 9
2.2.2 Definition of molecular properties 10
2.2.3 Density matrix formalism 11
2.2.4 Full expressions for hyperpolarizabilities 14
2.2.5 Classical orientational averaging 14

3 Computational methods **17**
3.1 Ab initio calculations 17
3.2 Born-Oppenheimer approximation 19
3.3 Electronic structure methods 19
3.3.1 Hartree-Fock method 19
3.3.2 Correlated methods 20
3.3.3 Density functional theory 21
3.4 Molecular properties 22
3.4.1 Electronic contributions 22
3.4.2 Vibrational contributions 23

4 Response theory **27**
4.1 Response functions 27
4.2 Response theory for an exact state 28
4.3 Molecular properties from response functions 29
4.3.1 Non-resonant properties 29

4.3.2 Excitation energies and residues 30
4.4 Response theory for an SCF reference state 30
4.5 Excited state gradient 32
4.6 Response theory beyond the random phase approximation 33

5 Two-photon absorption **35**
5.1 Two-photon absorption cross sections 37
5.2 Vibrational contributions 39
5.2.1 Zero-order harmonic approximation 39
5.2.2 Linear coupling model 40
5.2.3 Sum rules 41
5.3 One dimensional molecules 42
5.4 Few state models 44
5.5 Multi-branched molecules 45
5.6 Dynamics 49
5.6.1 Characteristic times 49
5.6.2 Modeling of nonlinear absorption 50
5.6.3 Saturation effects 51

6 Solvent effects **53**
6.1 Modeling strategies 54
6.2 Dielectric continuum models 55
6.2.1 Onsager reaction field model 56
6.2.2 Self-consistent reaction field model 60
6.3 Solvent effects on nonlinear optical properties 61
6.3.1 Definitions of the properties 61
6.3.2 Quantum mechanical models 62
6.3.3 Semiclassical model 63
6.3.4 Effective properties and local field factors 64
6.4 Examples of solvent effects on NLO properties 65
6.4.1 Saturation length of conjugated oligomers 65
6.4.2 Solvent effects on two-photon absorption 66

Summary **69**

Acknowledgments **71**

"Physics would be dull and life most unfulfilling if all physical phenomena around us were linear. Fortunately, we are living in a nonlinear world."

Y. R. Shen, *The Principles of Nonlinear Optics*

Chapter 1

Introduction

For a long time and for a large variety of phenomena it was believed that it was sufficient to consider the interaction of matter with optical fields or with electromagnetic fields as linear. The first experiment that showed a nonlinear interaction between electromagnetic fields and matter was performed by Kerr [1] who observed that birefringence was induced by a static electric field in a piece of glass. This happened at the end of the 19'th century and the effect he discovered was named after him.

The electric field intensities experienced by electrons in atoms and molecules are typically of the order of $10^{10} - 10^{12}$ V/m. The induced electronic polarization is then proportional to the powers of the ratio between the perturbing field and this atomic field. It generally takes at least 10^5 V/m to induce a pure nonlinear optical response in a medium[1]. This corresponds to about 2.5 kW/cm^2. Ordinary light sources are incoherent and too weak (for comparison - the light from the sun is of the order of 10^{-4} kW/cm^2). This is the reason that nonlinear effects in purely optical fields remained undiscovered until the first lasers appeared in the 1960's which provided sufficiently powerful and coherent light sources. Shortly after that, in 1961, Peter Franken with coworkers [2] observed second harmonic generation (frequency doubling) in a quartz crystal. It was the beginning of an entire new field in physics called nonlinear optics (NLO).

If the frequency of the light is close to any of the resonant frequencies (excitation energies) of the molecule an absorption of a photon can occur. In the case when the excitation energy in the molecule is twice the energy of incoming photons a simultaneous absorption of two photons (TPA) can take place. This effect of simultaneous absorption of two photons was theoretically predicted by Göppert-Mayer already in 1931 [3]. Also in this case the experimental observation had to wait until the invention of the laser 30 years later. The first experimental proof of two-photon absorption

[1]Lower intensities are sufficient for electro-optical effects where static or low frequency electric fields are used. The reason for this is that the electric field changes orientation of the prolonged molecules with highly anisotropic optical properties. A disadvantage is that a longer time is required for the response.

in the optical region was given by Kaiser and Garret in the spectrum of CaF_2:Eu^{3+} in 1961 [4].

Nonlinear optics has already become a basis for different technological areas. A large number of applications have been found in laser technologies utilizing the possibility of generation of the sum or difference of frequencies. This has, for example, enabled to produce tunable lasers in wide spectral regions. Another common everyday experience with nonlinear effects, although not purely optical, but electro-optical, are liquid crystal displays. Here, by modulating the electric field the molecules reorient and, due to their anisotropic optical properties, the overall optical characteristics are changed by the electric field. Yet another vast area of applications can be found in communication technologies, where electro-optical components transform the information transported by an optical field back into electric signals.

There are, however, many areas where nonlinear optics has not yet reached its full potential and much of the fundamental experimental and theoretical work needs still to be done. For instance all-optical switches would be very attractive in the communication technologies. There is a lot of excitement for *photonic* technologies in which photons are used for information transmission and manipulation, without resorting to conventional electronics.

The quadratic dependence on the field intensity of the two-photon absorption makes it suitable for applications like optical limitation for protection of sensors, or human eyes, against high intensity radiation, or like three dimensional imaging and data storage [5, 6, 7]. Another advantage of two-photon absorption is that it requires less energetical light to reach the same excitation level compared to one-photon absorption. Thus the two-photon laser scanning confocal microscopy would cause less damage to the biological samples because they are more tolerable to infrared (IR) light than to visible light. Also two-photon absorption might be used in photodynamic cancer therapy due to the better penetration of IR light through the skin than visible light.

All of these applications require materials with large two-photon absorption cross sections. Materials used for nonlinear optics have often been of crystal or semiconductor types. However, organic (or organometallic) materials also show promising features for this field. First, they are cheap to produce, and second, their properties can be well optimized by the proper use of functional groups which are sufficiently flexible. The understanding of structure-to-property relations in these molecules is crucial for in the design of new molecules with significant nonlinear optical properties.

Theoretical modeling provides important complements to experimental results. For the material design it can help to screen different types of molecules before they are synthesized. But more important - it can provide better understanding of the underlying mechanisms that determine or influence molecular properties. It might also provide information which is not accessible or which is very difficult to obtain experimentally. With the rapid development and increasing availability of computer

power the modeling is becoming more and more powerful.

From the theoretical point of view it is very appealing to make calculations on single isolated molecules which would experimentally correspond to dilute gas conditions. A vast number of studies and calculations ranging from highly accurate *ab initio* calculations for smaller molecules up to semiempirical calculations on big molecules have been performed. Different theoretical models for calculations of these properties have been introduced and various contributions to the nonlinear properties like electron correlation and molecular vibrations have been studied in detail.

However, life is not so simple, and most of the experiments, as well as technical applications, do not take place in the gas phase, but in solutions, matrices, thin films or in the solid phase. In condensed matter we deal typically with a number of particles of the order of Avogadros number - 10^{23}. The intermolecular distances are comparable to molecular dimensions and the interaction between the molecules cannot be neglected. The huge number of molecules or atoms involved results in a problem of great complexity, which creates a challenging field for development of new models and theories. These models need to be sufficiently simple to be computationally manageable but at the same time sufficiently accurate to adequately describe the most important physical processes. The approximations often seem to be crude, because there is always a trade off between accuracy and computational tractability.

There are several aspects of the role of a solvent environment on the molecular properties. First, the polarization of the medium affects the magnitude of the solute properties, but also the field experienced by the molecule. However, it is far from trivial to describe properly the local field acting on the molecule. The well known and widely used Lorentz-Lorenz factors are not always fully consistent with the advanced quantum mechanical models for calculating solute nonlinear properties. One of the reasons for this is that part of the polarization effect from the Lorentz-Lorenz local field factors has already been included in the effective Hamiltonian.

A second type of important solvent effects is the influence on the dynamics of the nonlinear absorption. Due to the perturbations by solvent molecules the dephasing times are much shorter than for the gas phase. In the case of absorption processes the short collisional dephasing time compared to the lifetime of the excited states involved enhances the off-resonant contributions to two-photon absorption. Especially for long pulses the measured two-photon absorption can be dominated by the incoherent two-step process.

In this work we consider electromagnetic fields as classical fields obeying Maxwell equations. This is justified since at the light intensities and frequencies we are interested in we deal with a huge number of photons, while the momentum of an individual photon is small compared to the momentum of a material system [8]. In contrast, we have to treat the single molecule quantum mechanically. In the present thesis we use response theory for calculating nonlinear optical properties within the *ab initio* framework.

We use the dielectric continuum model to treat the long range polarization effects

of the solvent environment. We generalize some of the simple models based on the Onsager reaction field model and address the issue of different possibilities of splitting this effect into the local field factors and change of the molecular properties. We derive connections between such different approaches together with the proper local field factors.

Among many nonlinear optical processes we focus mostly on the two-photon absorption processes. Structure to property relations, vibrational effects and effects of the solvent on the dynamics of populations of the excited states are analysed for two-photon absorption.

Chapter 2

Nonlinear optical processes

2.1 Macroscopic description

2.1.1 Electromagnetic fields

The theoretical descriptions of the classical electric and magnetic effects were beautifully united by J.C. Maxwell in 1864. These famous Maxwell equations fully describe the behavior of the electromagnetic fields in vacuum (in SI units)

$$\begin{aligned} \boldsymbol{\nabla}\cdot\mathbf{D} &= \rho, & \boldsymbol{\nabla}\cdot\mathbf{B} &= 0, \\ \boldsymbol{\nabla}\times\mathbf{E} + \frac{\partial\mathbf{B}}{\partial t} &= 0, & \boldsymbol{\nabla}\times\mathbf{H} - \frac{\partial\mathbf{D}}{\partial t} &= \mathbf{j}. \end{aligned} \tag{2.1}$$

Here $\rho, \mathbf{j}$ are charge and current density, respectively, and, for external sources in vacuum, $\mathbf{D} = \epsilon_0\mathbf{E}$ and $\mathbf{B} = \mu_0\mathbf{H}$. The existence of light - electromagnetic waves - follows directly from these equations.

Maxwell equations were formulated for the case of vacuum, but are still valid in the presence of matter for really microscopic fields rapidly varying in time and space. It turns out that it is possible to write equations similar to Maxwell equations in vacuum also for macroscopic fields, where the relationships between the $\mathbf{E}$ and $\mathbf{D}$ and between the $\mathbf{B}$ and $\mathbf{H}$ are modified due to the electric polarization $\mathbf{P}$ and magnetization $\mathbf{M}$

$$\mathbf{D} = \epsilon_0\mathbf{E} + \mathbf{P}, \qquad \mathbf{H} = \frac{1}{\mu_0}\mathbf{B} + \mathbf{M}. \tag{2.2}$$

The nonlinear optical processes we are dealing with are governed by electric fields since they have much stronger effects on electrons than the magnetic field in the same light beam (here we do not consider processes with external magnetic fields or circular dichroism effects).

All the quantities here - fields and polarizations - are in general functions of time and space. On the other hand, it is more convenient to work with their Fourier transformations and have the frequency and the wave vector as parameters. The wave vector dependence of the properties may play important roles in crystals. For example, a special requirement of so-called *phase-matching* conditions for the second harmonic generation can be understood as a momentum (wave vector) conservation. However, when dealing with molecules of sizes much smaller than the characteristic wavelength of the light it is only the frequency dependence of the quantities that is important. This is well justified for light in the visible region (380 - 720 nm) which we are mostly interested in and for typical molecules we consider (<10 nm).

For a set of a few monochromatic harmonic electric fields we can write $\mathbf{E}(t) = \sum_{s>0} \mathbf{E}^{\omega_s} cos(\omega_s t)$ as

$$\mathbf{E}(t) = \frac{1}{2} \sum_s \mathbf{E}^{\omega_s} e^{i\omega_s t}, \tag{2.3}$$

where we define $\mathbf{E}^{\omega - s} = \mathbf{E}^{\omega_s}$. Here we have written the summation over all frequencies explicitly. Nevertheless, in the rest of this chapter we use the Einstein summation convention where the repeated indices mean automatic summation.

2.1.2 Susceptibilities

The total polarization of the material can be split into linear and nonlinear parts

$$\mathbf{P} = \mathbf{P}^{\mathrm{L}} + \mathbf{P}^{\mathrm{NL}}. \tag{2.4}$$

In the linear regime the polarization oscillates at the same frequencies as the perturbing fields - just like a classical forced oscillator. However, if the light intensity is large, the nonlinear terms can become important and some combinations of the frequencies of the perturbing fields may therefore occur in the polarization.

In the range of field intensities we are interested in, the polarization of the material can be written in a perturbation expansion[1] in terms of the electric field intensity $\mathbf{E}$. The general expression in time and space domains would be

$$P_i(\mathbf{R}, t) = \int_{-\infty}^{t} dt' \int d^3R' \chi_{ij}^{(1)}(\mathbf{R}, t, \mathbf{R}', t') E_j(\mathbf{R}', t') \tag{2.5}$$
$$+\frac{1}{2} \int_{-\infty}^{t} dt' \int_{-\infty}^{t'} dt'' \int \int d^3R' d^3R'' \chi_{ijk}^{(2)}(\mathbf{R}, t, \mathbf{R}', t', \mathbf{R}'', t'') E_j(\mathbf{R}', t') E_k(\mathbf{R}'', t'')..., \tag{2.6}$$

where χ^1 and χ^2 are the first and second order susceptibilities. Since we often use only a few frequencies in the perturbing fields it is quite natural and much more

[1] For very high intensities this perturbation can break down. Examples are saturation effects in the absorption and electric breakdown of dielectric materials etc.

convenient to work in the frequency domain obtained by a Fourier transformation. For the spatial part the Fourier transformation would introduce wave vector (momentum) dependent quantities. In some systems with translational symmetry, like crystals, it is important to consider this wave vector dependence of the susceptibilities. However, when working with disordered molecules of sizes much smaller than the wave vector of the light we can neglect this dependence and focus only on the frequency dependence.

In the frequency domain the polarization expansion can be written as

$$\begin{aligned} P_i(\omega) &= \chi^{(1)}_{ij}(-\omega;\omega_s)E^{\omega_s}_j + \frac{1}{2}\chi^{(2)}_{ijk}(-\omega;\omega_s,\omega_t)E^{\omega_s}_j E^{\omega_t}_k + \\ &+ \frac{1}{3!}\chi^{(3)}_{ijkl}(-\omega;\omega_s,\omega_t,\omega_u)E^{\omega_s}_j E^{\omega_t}_k E^{\omega_u}_l + ..., \end{aligned} \tag{2.6}$$

where $\boldsymbol{\chi}^{(1)}(-\omega;\omega_s)$, $\boldsymbol{\chi}^{(2)}(-\omega;\omega_s,\omega_t)$ and $\boldsymbol{\chi}^{(3)}(-\omega;\omega_s,\omega_t,\omega_u)$ are the first, second and third order susceptibilities. These are in general anisotropic tensors. We should note that there exist nonvanishing contributions to P(ω) from $\boldsymbol{\chi}^{(n)}(-\omega;\omega_1,\omega_2,...\omega_n)$ only if $\omega = \omega_1 + \omega_2 + ...\omega_n$, which follows from the conservation of energy. Given these susceptibilities of the material we can model the time evolution and propagation of the macroscopic electromagnetic fields through the medium.

2.1.3 Non-resonant processes

If the frequency or the combination of the frequencies of the incoming light is far from any resonances (excitation energies) all the susceptibilities in (2.6) are real quantities. The energy is then transferred only between the different modes of the electromagnetic field, but not between field and matter. Such processes are called *non-resonant*.

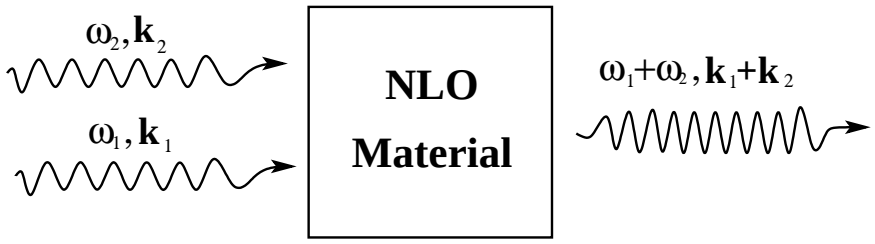

Figure 2.1: Sum frequency generation a from macroscopic point of view. The two light beams with frequencies ω_1, ω_2 give rise to the output field at the frequency $\omega_1+\omega_2$ due to the nonlinear optical medium.

An example of a *non-resonant* nonlinear optical process is the sum frequency generation (see Fig. 2.1). We consider here two incoming light beams with the frequencies

ω_1, ω_2. In the medium with a high second order susceptibility $\boldsymbol{\chi}^{(2)}$ a polarization at frequency $\omega = \omega_1 + \omega_2$ is induced. A macroscopic field at the sum of the frequencies appears if two conditions are satisfied: Conservation of energy and conservation of momentum. The conservation of energy is automatically satisfied, since the outgoing frequency ω is the sum of the frequencies of the incoming field. The conservation of momentum imposes a condition for the refractive indeces at frequencies ω_1, ω_2 and $\omega_1 + \omega_2$ (the so-called phase-matching conditions).

In the special case of sum frequency generation, when $\omega_1 = \omega_2$, the resulting sum frequency is $2\omega_1$ and therefore this process is called second harmonic generation (SHG). Examples of third order *non-resonant* nonlinear optical processes are third harmonic generation, intensity dependent refractive index and degenerate four-wave mixing [9, 10, 11].

2.1.4 Absorption processes

The rate of the time averaged energy absorbed by matter in the presence of electromagnetic fields is given by

$$\left\langle \frac{d}{dt}\left(\frac{\text{absorbed energy}}{\text{volume}}\right)\right\rangle = \langle \mathbf{jE} \rangle , \tag{2.7}$$

where $\mathbf{j}$ is the current density induced in the medium. We consider first the linear polarization of the medium $\mathbf{P}^{(1)}(t) = \boldsymbol{\chi}^{(1)}(-\omega;\omega)\mathbf{E}^{\omega}e^{-i\omega t}$, which gives

$$\mathbf{j} = \frac{\partial \mathbf{P}^{(1)}(t)}{\partial t} = -i\omega\boldsymbol{\chi}^{(1)}(-\omega;\omega)\mathbf{E}^{\omega}e^{-i\omega t}, \tag{2.8}$$

$$\left\langle \frac{d}{dt}\left(\frac{\text{absorbed energy}}{\text{volume}}\right)\right\rangle = \frac{1}{2}\omega Im\left[\chi^{(1)}_{ij}(-\omega;\omega)\right] E^{\omega}_i E^{\omega *}_j . \tag{2.9}$$

In the case of the third order polarization we have

$$P^{(3)}_i(t) = \frac{1}{8}\chi^{(3)}_{ijkl}(-\omega;\omega,\omega,-\omega)E^{\omega}_j e^{-i\omega t}E^{\omega}_k e^{-i\omega t}E^{\omega *}_l e^{i\omega t}, \tag{2.10}$$

$$j = \frac{\partial P}{\partial t} = \frac{1}{8}(-i\omega)\chi^{(3)}_{ijkl}\left(-\omega;\omega,\omega,-\omega\right) E^{\omega}E^{\omega}E^{\omega *}e^{-i\omega t}, \tag{2.11}$$

and the absorbed energy takes the form

$$\left\langle \frac{d}{dt}\left(\frac{\text{absorbed energy}}{\text{volume}}\right)\right\rangle = \frac{1}{16}\omega Im\left[\chi^{(3)}_{ijkl}\left(-\omega;\omega,\omega,-\omega\right)\right] E^{\omega}_i E^{\omega *}_j E^{\omega}_k E^{\omega *}_l . \tag{2.12}$$

This means that the absorbed energy is proportional to the square of the field intensity and that the two-photon absorption cross section is connected to the imaginary part of $\boldsymbol{\gamma}^{(3)}\left(-\omega;\omega,\omega,-\omega\right)$ (since $\chi^{(3)} = N\langle\gamma^{(3)}\rangle$).

2.2 Microscopic description

Another point of view on nonlinear optical phenomena is to see them as non-resonant light scattering by molecules. We consider here sum frequency generation with the input fields at frequencies ω_1 and ω_2 where both of these and their sum are far from any stationary state of the molecule. That means that these photons excite the molecule only into virtual non-stationary states. The lifetime of these virtual states is shorter as we are far from any real resonance, obeying the so-called time-energy uncertainty relation $\tau \Delta E \geq \frac{1}{2}\hbar$.

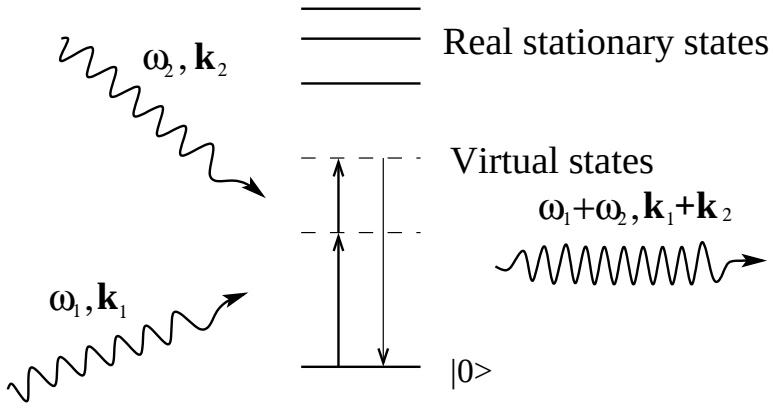

Figure 2.2: Sum frequency generation as a non-resonant light scattering. All the frequencies involved ω_1, ω_2 and $\omega_1 + \omega_2$ are far from real stationary states. The conservation of energy and conservation of momentum conditions have to be satisfied.

2.2.1 Interaction of light with molecules

This work is concerned with optical properties of molecules. Since the electric field in electromagnetic waves is interacting with molecules much stronger than the magnetic field, the phenomena we concentrate on here are of purely electric origin. At the microscopic level we focus on the behavior of the molecular dipole moment in the applied field, while on the macroscopic level it is the behavior of polarization (averaged density of dipole moments) we are concerned with.

We treat the molecule quantum mechanically while the electromagnetic radiation is treated classically. As we already mentioned in the introduction this is justified

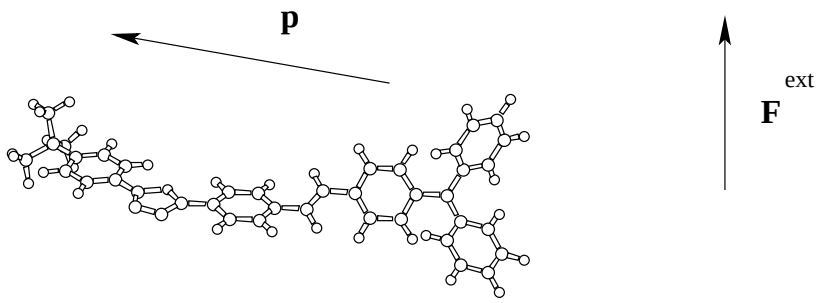

Figure 2.3: A molecule in a perturbing electric field.

since we deal with a huge number of photons, while each individual photon is carrying a small momentum compared to the momentum of a material system [8].

For a plane wave the spatial dependence of the electric field is $\propto e^{i\mathbf{kr}} = 1 - i\mathbf{kr}...$ The leading term in the expansion leads to the interaction Hamiltonian in the "dipole approximation"

$$H^{\text{int}} = -\hat{\boldsymbol{\mu}}\mathbf{F}(t), \tag{2.13}$$

where $\hat{\boldsymbol{\mu}}$ is the dipole moment operator and the $\mathbf{F}(t)$ is the oscillating electric field intensity. The second term in the expansion would introduce quadrupole coupling and so on. Since $k = \frac{2\pi}{\lambda}$ this approximation is justified for the cases $\frac{r}{\lambda} << 1$. For visible light with $\lambda \approx 380 - 720$ nm and molecules with lengths of a few nanometers (few 10's of Ångstroms) the dipole approximation is well justified[2].

2.2.2 Definition of molecular properties

The dipole moment of a molecule is of course influenced by the applied electric field. In the first approximation it depends linearly on the field intensity. For the isolated molecule with a fixed orientation we can write

$$p_i = \mu_i^0 + \alpha_{ij}^0 F_j, \tag{2.14}$$

where μ^0 is the permanent dipole moment of the unperturbed molecule and α^0 is the polarizability of the molecule. In fact, this is only an approximation and by applying very strong fields the dependence is no longer linear. It is very useful to write the dipole moment in terms of a Taylor expansion as first introduced by Buckingham [12]

$$p_i = \mu_i^0 + \alpha_{ij}^0 F_j + \frac{1}{2!}\beta_{ik}^0 F_j F_k + \frac{1}{3!}\gamma_{ik}^0 F_j F_k F_l + ..., \tag{2.15}$$

[2]The higher order terms may become important for example if the dipole transitions are symmetry forbidden.

where the coefficients in the expansion are the permanent dipole moment $\boldsymbol{\mu}^0$, polarizability $\boldsymbol{\alpha}^0$, first hyperpolarizability $\boldsymbol{\beta}^0$, second hyperpolarizability $\boldsymbol{\gamma}^0$, etc. An equivalent expansion can be obtained for the energy

$$E = E^0 + \mu_i^0 F_i + \frac{1}{2!}\alpha_{ij}^0 F_i F_j + \frac{1}{3!}\beta_{ik}^0 F_i F_j F_k + \frac{1}{4!}\gamma_{ik}^0 F_i F_j F_k F_l + ..., \tag{2.16}$$

where E_0 is the energy of the unperturbed molecule and all other coefficients are equal to the coefficients from (2.15). In this expansion the electric interaction energy (2.13) is included as well as the energy required to polarize the molecule. This formulation is more useful when properties are deduced from quantum mechanical calculations.

In the dynamic case it is very useful to decompose all the time dependent variables and properties like fields, dipole moments etc. into frequency dependent Fourier components. We can demonstrate this approach by a simple example when the applied field is composed from a static part $\mathbf{F}^0$ and a dynamic part $\mathbf{F}^\omega cos(\omega t)$ with certain frequency ω

$$F_i(t) = F_i^0 + F_i^\omega cos(\omega t). \tag{2.17}$$

We can decompose the fluctuating dipole moment $\mathbf{p}(t)$ from the latter equation into Fourier components

$$p_i(t) = p_i^0 + p_i^\omega cos(\omega t) + p_i^{2\omega} cos(2\omega t) + p_i^{3\omega} cos(3\omega t) + ..., \tag{2.18}$$

and define the frequency dependent hyperpolarizabilities in the Taylor convention to be the coefficients from the following expansions (see Willets *et. al.* [13] for more details)

$$p_i^0 = \mu_i^0 + \alpha_{ij}^0 F_j^0 + \frac{1}{2}\beta_{ijk}^0 F_j^0 F_k^0 + \frac{1}{4}\beta_{ijk}(0;\omega,-\omega) F_j^\omega F_k^\omega + ..., \tag{2.19}$$

$$\begin{aligned} p_i^\omega &= \alpha_{ij}(-\omega;\omega) F_j^\omega + \beta_{ijk}(-\omega;\omega,0) F_j^\omega F_k^0 + \frac{1}{2}\gamma_{ijkl}(-\omega;\omega,0,0) F_j^\omega F_k^0 F_l^0 \\ &+ \frac{1}{8}\gamma_{ijkl}(-\omega;-\omega,\omega,\omega) F_j^\omega F_k^\omega F_l^\omega + ..., \end{aligned} \tag{2.20}$$

$$p_i^{2\omega} = \frac{1}{4}\beta_{ijk}(-2\omega;\omega,\omega) F_j^\omega F_k^\omega + \frac{1}{8}\gamma_{ijkl}(-2\omega;\omega,\omega,0) F_j^\omega F_k^\omega F_l^0 + ..., \tag{2.21}$$

$$p_i^{3\omega} = \frac{1}{24}\gamma_{ijkl}(-3\omega;\omega,\omega,\omega) F_j^\omega F_k^\omega F_l^\omega + ... \tag{2.22}$$

2.2.3 Density matrix formalism

Although the time dependent Schrödinger equation (3.1) in principle provides the tool for calculating the time development of the quantum mechanical system, it is practically impossible to implement fully for very large disordered systems, like liquids. This is also not a very good idea since such systems behave in some sense

classically. Therefore, it is natural to attempt to describe at least a small subsystem of the whole system, e.g. molecule, quantum mechanically, while the effect of the other molecules should be included in some statistically averaged way. If, for the processes of interest, the relaxation effects caused by environment are important, it is more convenient to use the density matrix formalism than the Schödinger equation.

The density matrix operator can be written as

$$\hat{\rho} = |n\rangle W_n \langle n|, \tag{2.23}$$

where W_n is the probability that the molecule is in the pure state $|n\rangle$ of the unperturbed molecule. The time development of the density matrix is given by the Liouville equation

$$\frac{\partial \rho}{\partial t} = i\left[\rho, H\right] + \left\{\frac{\partial \rho}{\partial t}\right\}_R, \tag{2.24}$$

where H is the molecular Hamiltonian and $\left\{\frac{\partial \rho}{\partial t}\right\}_R$ represents the relaxation effect introduced by the stochastic nature of the interaction with the environment or spontaneous decay. The Hamiltonian of the molecule in the perturbing field can be written as

$$H = H_0 + H', \qquad H'(t) = h^s e^{-i\omega_s t}, \tag{2.25}$$

where H_0 is the unperturbed Hamiltonian and H' represents the interaction with the electromagnetic field. We use here and in the rest of this chapter the Einstein summation convention where the repeated indices mean automatic summation.

In the interaction picture with $\rho_I(t) = e^{iH_0 t}\rho_I(t)e^{-iH_0 t}$ we get

$$\frac{d\rho_I(t)}{dt} = i\left[\rho_I(t), H_I'(t)\right] - \left\{\frac{d\rho_I}{dt}\right\}_R. \tag{2.26}$$

A good description of the global damping is $\left\{\frac{d\rho_I}{dt}\right\}_R = \Gamma\rho_I$. The diagonal elements Γ_{ii} are related to the inversed lifetime of the population of the level i. The off-diagonal of Γ consists of the two qualitatively different contributions $\Gamma_{ii} + \Gamma_{jj}$ and γ_{ij}

$$\Gamma_{ij} = \frac{1}{2}\left(\Gamma_{ii} + \Gamma_{jj}\right) + \gamma_{ij}. \tag{2.27}$$

The first contribution comes from the decay rates Γ_{ii} and Γ_{jj} of levels i and j, while the second term γ_{ij} is caused by the dephasing collisions between the absorbing molecule and the solvent molecules and is proportional to the total concentration of the molecules in a solution. The dephasing is one of the main reasons for the large broadening of the spectral lines in a solvent environment.

The equation for the time development of the density matrix (2.26) is in general very difficult to solve analytically if more than two excited states are taken into account. One way is to try to make some approximations for the specific case, select a few important excited states and try to solve the problem numerically or, by certain approximations, analytically. Another approach is to use the perturbation expansion of the density matrix

$$\rho_I(t) = \rho_I^{(0)}(t) + \rho_I^{(1)}(t) + ... \tag{2.28}$$

This is relevant for the cases where we can expect quasi-stationary solutions. For non-resonant processes this is usually the case, but for resonant (absorption) processes where saturation effects might occur the perturbation expansion might break down completely. For many cases where the perturbation expansion is working we can obtain the recurrence expressions

$$\frac{d\rho_I^{(n)}(t)}{dt} = i\left[\rho_I^{(n-1)}(t), H_I'(t)\right] - \left\{\frac{d\rho_I^{(n)}}{dt}\right\}_R, \tag{2.29}$$

which leads to the following solutions

$$\rho_{Inm}^{(1)}(t) = \left(\rho_{mm}^{(0)} - \rho_{nn}^{(0)}\right)\frac{h_{nm}^s}{\omega_s - \omega_{nm} + i\Gamma_{mn}} e^{-i(\omega_s - \omega_{nm})t}, \tag{2.30}$$

$$\begin{aligned}\rho_{Inm}^{(2)}(t) &= \left\{\left(\rho_{mm}^{(0)} - \rho_{oo}^{(0)}\right)\frac{h_{no}^s h_{om}^t}{\omega_t - \omega_{om} + i\Gamma_{mn}}\right. \\ &- \left.\left(\rho_{oo}^{(0)} - \rho_{nn}^{(0)}\right)\frac{h_{no}^s h_{om}^t}{\omega_t - \omega_{nm} + i\Gamma_{mn}}\right\}\frac{e^{-i(\omega_s+\omega_t-\omega_{nm})t}}{\omega_s + \omega_t - \omega_{nm} + i\Gamma_{nm}},\end{aligned} \tag{2.31}$$

$$\begin{aligned}\rho_{Inm}^{(3)}(t) &= \left\{\left(\rho_{mm}^{(0)} - \rho_{oo}^{(0)}\right)\frac{h_{np}^u h_{po}^s h_{om}^t}{(\omega_s + \omega_t - \omega_{pm} + i\Gamma_{pm})(\omega_t - \omega_{om} + i\Gamma_{om})}\right. \\ &- \left(\rho_{oo}^{(0)} - \rho_{pp}^{(0)}\right)\frac{h_{np}^u h_{po}^t h_{om}^s}{(\omega_s + \omega_t - \omega_{pm} + i\Gamma_{pm})(\omega_t - \omega_{po} + i\Gamma_{po})} \\ &+ \left(\rho_{pp}^{(0)} - \rho_{oo}^{(0)}\right)\frac{h_{np}^s h_{po}^t h_{om}^u}{(\omega_s + \omega_t - \omega_{no} + i\Gamma_{no})(\omega_t - \omega_{po} + i\Gamma_{po})} \\ &- \left.\left(\rho_{nn}^{(0)} - \rho_{pp}^{(0)}\right)\frac{h_{np}^t h_{po}^s h_{om}^u}{(\omega_s + \omega_t - \omega_{no} + i\Gamma_{no})(\omega_t - \omega_{np} + i\Gamma_{np})}\right\} \\ &\times \frac{e^{-i(\omega_s+\omega_t+\omega_u-\omega_{nm})t}}{\omega_s + \omega_t + \omega_u - \omega_{nm} + i\Gamma_{nm}}.\end{aligned} \tag{2.32}$$

Once the density matrix is known, the mean value of any operator of the system is determined by the trace of the product of the operator and the density matrix

$$\langle A\rangle = Tr(\rho_I A_I) = Tr(\rho A). \tag{2.33}$$

2.2.4 Full expressions for hyperpolarizabilities

Since the molecular electronic excitation energies are much higher than the thermal energy (a few eVs compared to $kT \approx 0.025eV$) the molecules can be assumed to be in their ground electronic state $|0\rangle$ ($\rho^{(0)}_{nm} = \delta_{n0}\delta_{m0}$).

We can use these expressions for the expectation value of the dipole moment and the perturbation operator (2.13). Comparing it with the definitions of the polarizabilities and hyperpolarizabilities (2.19) - (2.22) we get

$$\alpha_{ij}(-\omega_\sigma;\omega_1) = \left\{ \frac{\langle n|\mu_i|m\rangle\langle m|\mu_j|n\rangle}{\omega_{mn} - \omega_1 - i\Gamma_{mn}} + \frac{\langle n|\mu_j|m\rangle\langle m|\mu_i|n\rangle}{\omega_{mn} + \omega_1 + i\Gamma_{mn}} \right\} \rho^{(0)}_{nn}, \tag{2.34}$$

$$\begin{aligned} \beta_{ijk}(-\omega_\sigma;\omega_1,\omega_2) &= \frac{1}{2!}\sum_{\mathcal{P}} \left\{ \frac{\langle n|\mu_i|m\rangle\langle m|\mu_j|o\rangle\langle o|\mu_k|n\rangle}{(\omega_{mn} - i\Gamma_{mn} - \omega_1 - \omega_2)\,(\omega_{on} - i\Gamma_{on} - \omega_2)} \right. \\ &+ \frac{\langle n|\mu_j|m\rangle\langle m|\mu_i|o\rangle\langle o|\mu_k|n\rangle}{\omega_{om} - i\Gamma_{om} - \omega_1 - \omega_2} \left[\frac{1}{\omega_{mn} + i\Gamma_{mn} - \omega_1} - \frac{1}{\omega_{on} + i\Gamma_{on} - \omega_2} \right] \\ &+ \left. \frac{\langle n|\mu_j|m\rangle\langle m|\mu_k|o\rangle\langle o|\mu_i|n\rangle}{(\omega_{mn} - i\Gamma_{mn} + \omega_1)\,(\omega_{on} - i\Gamma_{on} + \omega_1 + \omega_2)} \right\} \rho^{(0)}_{nn}, \end{aligned} \tag{2.35}$$

$$\begin{aligned} \gamma_{ijkl}(-\omega_\sigma;\omega_1,\omega_2,\omega_3) &= \frac{1}{3!}\sum_{\mathcal{P}} \left\{ \frac{\langle n|\mu_i|m\rangle\langle m|\mu_j|o\rangle\langle o|\mu_k|p\rangle\langle p|\mu_l|n\rangle}{(\omega_{mn} - i\Gamma_{mn} - \omega_\sigma)\,(\omega_{on} - i\Gamma_{on} - \omega_2 - \omega_3)\,(\omega_{pn} - i\Gamma_{pn} - \omega_3)} \right. \\ &- \frac{\langle n|\mu_j|m\rangle\langle m|\mu_i|o\rangle\langle o|\mu_k|p\rangle\langle p|\mu_l|n\rangle}{\omega_{mp} - i\Gamma_{mp} - \omega_1 - \omega_2 - \omega_3} \left[\frac{1}{(\omega_{on} - i\Gamma_{on} - \omega_2 - \omega_3)\,(\omega_{pn} - i\Gamma_{pn} - \omega_3)} \right. \\ &+ \left. \frac{1}{\omega_{op} - i\Gamma_{op} - \omega_2 - \omega_3} \left(\frac{1}{\omega_{on} - i\Gamma_{on} - \omega_2} - \frac{1}{\omega_{pn} - i\Gamma_{pn} - \omega_3} \right) \right] \\ &- \frac{\langle n|\mu_j|m\rangle\langle m|\mu_k|o\rangle\langle o|\mu_i|p\rangle\langle p|\mu_l|n\rangle}{\omega_{om} + i\Gamma_{om} + \omega_1 + \omega_2 + \omega_3} \left[\frac{1}{(\omega_{on} + i\Gamma_{on} + \omega_2 + \omega_3)\,(\omega_{pn} - i\Gamma_{pn} + \omega_3)} \right. \\ &+ \left. \frac{1}{\omega_{mp} - i\Gamma_{mp} - \omega_2 - \omega_3} \left(\frac{1}{\omega_{pn} + i\Gamma_{pn} - \omega_3} - \frac{1}{\omega_{mn} - i\Gamma_{mn} - \omega_1} \right) \right] \\ &+ \left. \frac{\langle n|\mu_j|m\rangle\langle m|\mu_k|o\rangle\langle o|\mu_l|p\rangle\langle p|\mu_i|n\rangle}{(\omega_{mn} + i\Gamma_{mn} + \omega_1)\,(\omega_{on} + i\Gamma_{on} + \omega_1 + \omega_2)\,(\omega_{pn} + i\Gamma_{pn} + \omega_\sigma)} \right\} \rho^{(0)}_{nn}, \end{aligned} \tag{2.36}$$

where $\omega_\sigma = \omega_1 + \omega_2$ for the first hyperpolarizability $\beta(-\omega_\sigma;\omega_1,\omega_2)$ and $\omega_\sigma = \omega_1 + \omega_2 + \omega_3$ for the second hyperpolarizability $\gamma(-\omega_\sigma;\omega_1,\omega_2,\omega_3)$. $\sum_{\mathcal{P}}$ denotes the summation of all terms obtained by permutation of the pairs $(i,\omega_\sigma),(j,\omega_1)$... For more details see e.g. ref. [14].

We can notice that at certain frequencies the real part of the denominators vanishes. In these cases we have resonant effects. If $\omega_1 = \omega_{mn}$ for certain n and m we have one-photon absorption taking place. For γ however, we receive resonances also for the case if the sum of two frequencies (e.g. $\omega_2 + \omega_3$) equals an energy difference between some two states. In this case two-photon absorption takes place. There are some resonances in β as well but these do not correspond to any real absorption.

2.2.5 Classical orientational averaging

Our description of molecular properties was so far connected to the fixed molecular positions and orientations. These are the microscopic properties of the molecules.

What is relevant to the measurement is a polarization - an averaged dipole moment of an ensemble of a large number of molecules. On the macroscopic scale we thus talk about "polarization" instead of "dipole moment" and about "linear and nonlinear susceptibilities" instead of "polarizability"' and "hyperpolarizabilities". We will discuss about the other effects of the molecular environment on the properties and local field factors in later chapters. Here we describe the effect of the orientational averaging. For more details on this issue see e.g. the review by Bishop [15].

The polarization of a gas can be written as

$$P_i = N\langle\mu_i\rangle, \tag{2.37}$$

where N is the density, and $\langle\mu_i\rangle$ means the thermal average of the dipole moment. Using a Boltzmann distribution function we can express the average in the form

$$\langle\mu_i\rangle = \frac{\int_0^{2\pi}\int_0^{\pi}(\mu_i e^{\frac{-\Delta E}{kT}})\sin\theta d\theta d\phi}{\int_0^{2\pi}\int_0^{\pi}\sin\theta d\theta d\phi}, \tag{2.38}$$

where k is Boltzmann constant and T is the temperature. The interaction energy ΔE can be written as

$$\Delta E = -\mu_i F_i, \tag{2.39}$$

for a static field F. The Boltzmann statistical distribution is valid for the equilibrium case, that means when a static field is applied. The optical fields on the other hand have frequencies too high for the molecules to follow with their rotational and translational degrees of freedom. Thus the ΔE entering the average (2.38) is just dependent on the static component of the perturbing field.

For the gas phase the susceptibilities would, of course, turn out to be scalar quantities due to the averaging (2.38) and the symmetry of the problem. However, for condensed matter these quantities could become anisotropic since ΔE (2.39) will be modified due to the specific interactions among the molecules.

As an example we can show the expression for the static linear susceptibility, which, after averaging, is found to be approximately [16, 8]

$$\chi^1_{ZZ} = N\left(\overline{\alpha}_{ZZ} + \frac{\mu^2}{3kT}\right), \qquad \overline{\alpha}_{ZZ} = \frac{1}{3}\left(\alpha_{xx} + \alpha_{yy} + \alpha_{zz}\right), \tag{2.40}$$

where N is the particle density, Z corresponds to the laboratory coordinate system, and x,y, and z correspond to the molecular coordinate system. The second term originates from thermal averaging of the dipole moment orientation. The approximation leading to Eq. (2.40) is based on the fact that for usual situations the ratio $\frac{F\mu}{kT} << 1$ and thus the exponential function in Eq. (2.38) can be approximated by the first two terms in the expansion $e^{-\frac{F\mu}{kT}} = 1 - \frac{F\mu}{kT} + ...$ The Langevin function representing the exact integration could be replaced by a linear function in this region, see for example

Böttcher [16] for a more detailed analysis. At normal temperatures and typical values of the dipole moment this approximation is well justified for the fields below 10^6 V/cm. The consequence of the fact that for real situations the ratio $\frac{F\mu}{kT}$ is much smaller than 1 is that the molecules are oriented in the gas phase almost entirely randomly even when external fields are applied. Only after averaging over a large number of molecules the net polarization occurs.

After orientational averaging, the temperature independent terms for the hyperpolarizabilities read

$$\langle\beta\rangle_{ZZZ} = \frac{1}{5}\left(\beta_{zii} + \beta_{izi} + \beta_{iiz}\right), \tag{2.41}$$

$$\langle\beta\rangle_{XXZ} = \frac{1}{5}\left(2\beta_{zii} - 3\beta_{izi} + 2\beta_{iiz}\right), \tag{2.42}$$

$$\langle\gamma\rangle_{ZZZZ} = \frac{1}{15}\left(\gamma_{iijj} + \gamma_{ijij} + \gamma_{iijj}\right), \tag{2.43}$$

$$\langle\gamma\rangle_{ZXXZ} = \frac{1}{30}\left(4\gamma_{ijji} - \gamma_{ijij} - \gamma_{iijj}\right). \tag{2.44}$$

An important point to observe is that when optical fields are applied, then the orientational degrees of freedom cannot follow the rapid changes of the field and thus the temperature dependent term in equation (2.40) disappears. That means that for polar molecules the static susceptibility could be much higher than the dynamic one, while for nonpolar molecules static and dynamic susceptibilities would be more or less the same. That is because the change for nonpolar molecules would be caused exclusively by the dispersion of electronic polarizability α^{e} which is usually not very dramatic for the non-resonant case (energy of photons much below the electronic transition energies). Although for liquids the discussion is a little bit more complicated, the basic ideas are similar and we can see this behavior for example for water, which is a highly polar molecule, where the static permitivity is 78.5, while the dynamic permitivity is 1.78, and benzene, which is nonpolar, where both the static and dynamic permitivities are around 2.28.

Chapter 3

Computational methods

3.1 Ab initio calculations

A detailed understanding of the structure, properties and behavior of atoms and molecules is based on the ideas of quantum mechanics developed at the beginning the 20th century. The fundamental starting point for all the nonrelativistic *ab initio* computational methods is the Schrödinger equation. For the molecule itself the use of quantum mechanics is inevitable while for the perturbing electromagnetic field a classical description is in most cases sufficient.

For isolated molecules the Schrödinger equation may be written as

$$H\Psi = i\frac{\partial \Psi}{\partial t}, \tag{3.1}$$

where Ψ is the time-dependent complex many particle wave function, and H is the Hamiltonian (in atomic units)

$$\begin{aligned} H &= -\sum_A \frac{1}{2M_A}\nabla_A^2 + \sum_{B>A}\sum_A \frac{Z_A Z_B}{R_{AB}} \\ &\quad -\sum_i \frac{1}{2}\nabla_i^2 - \sum_i \sum_A \frac{Z_A}{R_{Ai}} + \sum_{j>i}\sum_i \frac{1}{r_{ij}} \end{aligned} \tag{3.2}$$

where i, j refers to electrons, A, B to nuclei. A wave function Ψ that depends on all the nuclear and electronic coordinates and time is impossible to calculate analytically for anything containing more than one electron and one proton. We have to do some very basic approximations in order to be able to calculate quantitative results but also to get a qualitative feeling for the problems.

In this thesis we have chosen *ab initio* methods as the framework for the calculations of molecular nonlinear optical properties. In these methods we make approximations to the wave functions, but keep the Hamiltonian in principle exact, meaning

that we project the Hamiltonian on a set of orbitals and solve the projected problem exactly. An overview on *ab initio* computational methods used nowadays can be found in many textbooks [17, 18, 19]. An alternative would be *semi-empirical methods* where some effective Hamiltonian is used and where parameters are fitted from experimental (usually spectroscopic) data.

One of the basic approximations used in *ab initio* calculations is the separation of the electronic and vibrational wave functions - the Born-Oppenheimer approximation. Since electrons are fermions, the electronic wave function has to be totally antisymmetric with respect to interchange of the coordinates of any two electrons with the same spin. Any such many electron wave function can be expressed as the sum of single determinants constructed from the set of one electron molecular orbitals. There are naturally two directions of approximating the electronic wave function :

i, the one-electron molecular orbitals are expressed as a linear combination of a finite number of basis functions;

ii, the expansion in many-electron space using a truncated set of determinants.

The simplest electronic wave function with the correct symmetry is the so-called Hatree-Fock wave function, which is just a single determinant constructed from molecular orbitals.

In the treatment of the vibrational wave function the electronic energy together with nuclear repulsion energy serves as the potential energy surface on which the nuclei move. The starting point of any further approximation is the so-called harmonic approximation. In this approximation the potential surface is approximated by a quadratic function in terms of nuclear coordinates. The resulting vibrational wave function is a product of single harmonic oscillators. Any anharmonicity of the potential surface mixes these oscillators.

Since we are focusing on closed shell molecules containing relatively light elements, the Hartree-Fock wave function obtained by solving a non-relativistic Schrödinger equation for a determinant of orbitals is usually a reasonably good approximation. It is also a method which can be applied for relatively large molecules. It is not a highly accurate method but the response function based on Hartree-Fock wave function (random phase approximation) can provide reasonable accuracy for our purposes - namely the calculation of nonlinear optical properties of molecules.

The basis set requirements for calculations are much dependent on the method, the molecule and the properties of interest. The highly correlated methods have the strongest demand on the quality of the basis set, and non-linear properties like hyperpolarizabilities are usually more sensitive to the basis set expansion than linear properties.

3.2 Born-Oppenheimer approximation

Due to the large difference in mass of nuclei and electrons we can expect the electrons to move much faster. In fact, this turns out to motivate a very useful approximation of separation of electronic and nuclear degrees of freedom known as the *Born-Oppenheimer approximation* . It means that we write the total wave function as a product of the electronic and nuclear wave functions

$$\Psi(\mathbf{R},\mathbf{r}) = \Psi^{el}(\mathbf{r};\mathbf{R})\Psi^{nuc}(\mathbf{R}), \tag{3.3}$$

where the electronic wave function $\Psi^{el}(\mathbf{r};\mathbf{R})$ depends on the nuclear positions $\mathbf{R}$ only parametrically. First solving the Schrödinger equation for the electronic part gives us the electronic energy for a particular nuclear geometry. The sum of the electronic energy and the nuclear repulsion energy can then be used as a potential energy surface in the equation for the nuclear wave function.

3.3 Electronic structure methods

3.3.1 Hartree-Fock method

Since electrons are fermions, the electronic wave function Ψ^{el} depending on all the electronic coordinates (spatial and spin) and time has to be antisymmetric with respect to interchange of any two electrons (Pauli exclusion principle). The simplest form which satisfies this requirement is the Slater determinant formed out of one-electron functions. This approximation is the basis of the *Hartree-Fock wave function*. For N electrons it reads

$$\Psi^{Hartree-Fock} = \frac{1}{\sqrt{N!}}\begin{vmatrix} \chi_1(\mathbf{x}_1) & \chi_1(\mathbf{x}_2) & ... & \chi_1(\mathbf{x}_N) \\ \chi_2(\mathbf{x}_1) & \chi_2(\mathbf{x}_2) & ... & \chi_2(\mathbf{x}_N) \\ \vdots & \vdots & & \vdots \\ \chi_N(\mathbf{x}_1) & \chi_N(\mathbf{x}_2) & ... & \chi_N(\mathbf{x}_N) \end{vmatrix}, \tag{3.4}$$

where $\chi_1, \chi_2, ..., \chi_N$ are the one-electron molecular spin orbitals, and where $\mathbf{x}_i$ is the collective notation for the spatial and spin coordinates of the i-th electron.

The *variational principle* states that the best approximation to the exact solution of the Schrödinger equation for a certain type of trial function is the one that gives the minimal (or stationary) energy with respect to the variation of all the parameters it contains. If we write the molecular orbitals as a linear combination of atomic orbitals and apply the *variational principle* we receive the equations for the coefficients determining the molecular orbitals. The energetic contribution of the electron in a

single orbital to the total energy is such as if the electron was exposed to the averaged electric field of all the other electrons. This averaged field is obtained *self-consistently* with the determination of the molecular orbitals. Therefore this approximation for the wave function is also called the *self-consistent field* (SCF) approximation.

3.3.2 Correlated methods

In the Hartree-Fock wave function the electrons are moving in the "averaged" field of all other electrons. This description is lacking the correlation of the motion of the electrons.

The Hartree-Fock wave function is evidently only an approximation to the exact wave function since it is restricted to one Slater determinant. On the other hand, any antisymmetric wave function can be written as a sum of Slater determinants. The most general of the methods for treatment of *correlation* effects use a truncated expansion of the wave function with several Slater determinants.

As a result of the Hatree-Fock calculation we receive the occupied orbitals and a set of unoccupied orbitals. The easiest way to write a correlated wave function is to to use a linear combination of the determinants based on Hartree-Fock orbitals with some occupied spin orbitals replaced by unoccupied spin orbitals

$$|\Psi\rangle = c_0|\Psi_0\rangle + \sum_{ia} c_a^i|\Psi_a^i\rangle + \sum_{\substack{b>a \\ j>i}} c_{ab}^{ij}|\Psi_{ab}^{ij}\rangle + ..., \tag{3.5}$$

where the a, b mean unoccupied spin orbitals, r, s occupied spin orbitals, c are the coefficients and $|\Psi_a^i\rangle$ represents the determinant where an occupied spin orbital χ_i is replaced by the unoccupied spin orbital χ_a. Using the variational principle for obtaining the coefficients in front of the determinants we receive the so-called configuration interaction (CI) method.

If we at the same time optimize the molecular orbitals we receive the multiconfigurational self-consistent field (MCSCF) method. This method is useful especially in the cases where the HF wave function is a bad approximation. That happens in situations when there is strong so-called static correlation, often originating from near degeneracy of configurations, occurring e.g. when chemical bonds break or at transition or excited states.

There are different ways of selecting which determinants should be included in the wave function expansion. We can define the set of orbitals within which all the excitations and de-excitations would be allowed - a so-called complete active space (CAS). A different way is to select more groups of orbitals and restrict the number of excitations and de-excitations for each group - a so-called restricted active space (RAS).

A better way of combining the excited determinants in the expansion than in CI is the use of exponential parametrization with excitation operators. The so-called cou-

pled cluster (CC) wave functions are based on such an exponential parametrization

$$|\Psi^{CC}\rangle = e^{T_1+T_2+..T_n}|\Psi_0\rangle, \tag{3.6}$$

where the T_1 is the operator for single excitations, T_2 for double excitations etc. Usually only double and selected triple excitations are included. The coupled cluster wave functions are very popular for accurate calculations nowadays in the cases where HF is a good starting point.

A different way is to split the molecular Hamiltonian into the exactly soluble part and a perturbation. This is the basis for perturbation theory, in particular for the popular Møller-Pleset theory (MP) which is especially widely used in the second order (MP2).

3.3.3 Density functional theory

In recent years it has became very popular to use alternative approaches for treating electron exchange and correlation. Instead of using the wave function one works with the total electron density accounting for a theorem that states that the total energy is a unique functional of this electron density. A main advantage of this method is that it is much faster than other methods going beyond the Hartree-Fock approximation.

If the number of electrons is N, then the electron density is defined as

$$\rho(\mathbf{r}) = N \int ... \int |\psi|^2 ds_1 d\mathbf{x}_2 ... d\mathbf{x}_N. \tag{3.7}$$

If the exact electron density is known then at the positions of the cusps there are nuclei. And furthermore, from the value of $|\rho(\mathbf{r})|$ at the positions of the nuclei we can obtain the nuclear charge. Thus the full Hamiltonian would be known and hence in principle everything is known to set up the Schrödinger equation. This means that the knowledge of electron density is in principle all that is necessary for a complete determination of the molecular properties.

The first Hohenberg-Kohn theorem [20] shows that the knowledge of density also uniquely determines the external potential. The second Hohenberg-Kohn theorem allows us to introduce the variational principle, although only for the ground state.

Kohn and Sham [21] introduced the orbitals ϕ_i, which give the electron density as

$$\rho(\mathbf{r}) \quad = \quad \sum_{i=1}^{N} |\phi_i(\mathbf{r})|^2. \tag{3.8}$$

Using the variational principle we can derive the Kohn-Sham equations for the orbitals ϕ_i

$$\left[-\frac{1}{2}\nabla^2 + v(\mathbf{r}) + \int \frac{\rho(\mathbf{r}')}{|\mathbf{r}-\mathbf{r}'|} d\mathbf{r}' + v^{\mathrm{xc}}(\mathbf{r}) \right] \phi_i(\mathbf{r}) \quad = \quad \epsilon_i \phi_i(\mathbf{r}), \tag{3.9}$$

where the $v^{\mathrm{xc}}(\mathbf{r})$ is the exchange-correlation potential obtained as the functional derivative of the exchange-correlation energy $v^{\mathrm{xc}}(\mathbf{r}) = \frac{\delta E^{\mathrm{XC}}}{\delta \rho(\mathbf{r})}$.

3.4 Molecular properties

3.4.1 Electronic contributions

The basic methods for calculation of linear and non-linear properties, like the electronic polarizability and hyperpolarizabilities, are the following:

1. **Sum-over-states method.** This approach is based on the explicit summation over the excited states in the formulas (4.15)-(4.17). It is computationally very expensive for *ab initio* calculations due to the large number of states included in the summations. This approach is more interesting for semi-empirical calculations and very important from the point of view of interpretation.

2. **Few states method.** For some molecular systems the optical properties are dominated by a few electronic states which could be used to reduce the sum-over-states approach to a manageable extent.

3. **Finite field method.** Here the starting point is the energy expansion (2.16) where the total energy is calculated for different applied finite fields. The properties are then extracted by numerical differentiation. The disadvantages of this method are first, that it is only applicable to static fields and, second, that the applied finite field has to be carefully chosen in order to avoid numerical instabilities.

4. **Analytic derivative method.** Analytical derivatives are clearly less computationally expensive than the sum-over-states approach, but can still handle only static perturbations.

5. **Response theory method.** This is a very general approach that can handle also dynamic perturbations in an efficient and computationally tractable manner. The explicit summation over all excited states is reformulated into a problem of solving matrix equations without explicitly constructing the excited states [22, 23].

6. **The quasi-energy method.** This method provides a very general tool by means of which also frequency dependent properties can be obtained through analytic derivative techniques [24].

The calculations performed in this thesis make use of response theory and an SCF reference wave function. It is generally referred to as the random phase approximation (RPA), or equivalently, the time-dependent Hartree-Fock (TDHF) method.

3.4.2 Vibrational contributions

The simplest approximation for the potential energy surface is to make a quadratic expansion of the surface around the equilibrium geometry. This so-called harmonic approximation usually provides a very good starting point for any further calculations of vibrational effects.

We describe now a typical way of calculating the vibrational contributions to NLO properties by considering the polarizability. For the hyperpolarizabilities the vibrational contributions can be treated using the same ideas. The vibrational contributions to the resonant processes like two-photon absorption are described in chapter 5.

The explicit summation over vibrational states gives for the polarizability

$$\alpha_{ij}(-\omega;\omega) = \sum_{\mathcal{P}} \sum_{K,k} \frac{\langle 0,0^{\mathrm{v}}|\mu_i|K,k\rangle\langle K,k|\mu_j|0,0^{\mathrm{v}}\rangle}{\omega_K + \omega_k - \omega}, \tag{3.10}$$

where μ is the total dipole moment operator, K and k are the intermediate electronic and vibrational states, respectively. The ground electronic state is denoted as 0 and the ground state vibrational state 0^{v}. In the denominators ω_K and ω_k are the differences between the ground and excited state electronic and vibrational energies, respectively.

We can split this summation into two terms. One in which $K \neq 0$ and a second in which $K = 0$

$$\begin{aligned} \alpha_{ij}(-\omega;\omega) &= \sum_{\mathcal{P}} \sum_{K\neq 0,k} \frac{\langle 0,0^{\mathrm{v}}|\mu_i|K,k\rangle\langle K,k|\mu_j|0,0^{\mathrm{v}}\rangle}{\omega_K + \omega_k - \omega} \\ &+ \sum_{\mathcal{P}} \sum_{k} \frac{\langle 0,0^{\mathrm{v}}|\mu_i|0,k\rangle\langle 0,k|\mu_j|0,0^{\mathrm{v}}\rangle}{\omega_k - \omega}. \end{aligned} \tag{3.11}$$

We can assume that the energies belonging to electronic transitions are much higher than those belonging to vibrational transitions, i.e. $\omega_K >> \omega_k$ so ω_k in the denominator of the second term can be neglected (for non-resonant process we implicitly assume that ω is far from any electronic level). Then, using the closure formula for all the vibrational states belonging to the n'th electronic state $\sum_k |k\rangle\langle k| = 1$, the expression is simplified to

$$\alpha_{ij}(-\omega;\omega) = \sum_{\mathcal{P}} \sum_{\mathcal{P}} \sum_{K\neq 0} \langle 0^{\mathrm{v}}| \frac{\langle 0|\mu_i|K\rangle\langle K|\mu_j|0\rangle}{\omega_K - \omega} |0^{\mathrm{v}}\rangle + \sum_k \frac{\langle 0^{\mathrm{v}}|\mu_i|k\rangle\langle k|\mu_j|0^{\mathrm{v}}\rangle}{\omega_k - \omega}. \tag{3.12}$$

The first term here describes the vibrationally averaged electronic polarizability and the second term expresses the pure vibrational contributions. Thus the total polarizability can be written as

$$\alpha_{ij} = \alpha_{ij}^{\mathrm{e}} + \alpha_{ij}^{\Delta\mathrm{ZPVA}} + \alpha_{ij}^{\mathrm{v}}, \tag{3.13}$$

where the electronic contribution, which is usually dominant, is given by

$$\alpha^e_{ij}(-\omega;\omega) = \sum_{K\neq 0}\left[\frac{\langle 0|\mu_i|n\rangle\langle K|\mu_j|0\rangle}{\omega_K-\omega}+\frac{\langle 0|\mu_j|n\rangle\langle K|\mu_i|0\rangle}{\omega_K+\omega}\right]. \quad (3.14)$$

Here the sum goes over all electronic states and is evaluated at the equilibrium geometry.

Harmonic approximation and normal coordinates

In the Born-Oppenheimer approximation we describe the motion of the nuclei by the nuclear Schrödinger equation in which the electronic energy is forming a potential energy surface $V(\mathbf{R})$ in which the nuclei move. The equilibrium geometry is by definition such that this potential energy is minimal, thus the first derivative vanishes. Close to the equilibrium geometry the potential energy surface can be expanded into the quadratic term

$$V^{\text{nuc}} = V(\mathbf{R}_0)+\frac{1}{2}\sum_{A,B}\frac{\partial^2 V(\mathbf{R})}{\partial R_A \partial R_B}R_A R_B. \quad (3.15)$$

We know that the kinetic energy of the nuclei is given by

$$T^{\text{nuc}} = \frac{1}{2}\sum_A M_A \dot{R}_A^2. \quad (3.16)$$

First we can include the $\sqrt{M_A}$ term into R_A to get the mass weighted coordinates. We should also note that the potential energy cannot depend on the translation and rotation of the whole molecule. We can now introduce new coordinates by the linear transformation of these coordinates in such a way that we shall diagonalize also the potential energy while keeping the kinetic energy diagonal. These new coordinates are called normal coordinates

$$V^{\text{nuc}} = V_0+\frac{1}{2}\sum_a \omega_a^2 Q_a^2, \qquad T^{\text{nuc}}=\frac{1}{2}\sum_a \dot{Q}_a^2. \quad (3.17)$$

The normal coordinates represent a very good starting point for the description of molecular vibrational effects because in these coordinates the molecular vibrational wave function separates completely into a product of single harmonic oscillator wave functions.

Pure vibrational contributions

The pure vibrational contributions to the polarizability can be evaluated by expanding the dipole moment $\mu_i = \langle 0|\mu_i|0\rangle$ in the normal coordinates Q_a

$$\mu_i(\mathbf{Q}) = \mu_i(\mathbf{0})+\sum_a \frac{\partial \mu_i}{\partial Q_a}Q_a + ... \quad (3.18)$$

where the summation goes over all the normal modes. By assuming the harmonic approximation, that is a quadratic form of the electronic potential surfaces of the ground state, and by taking only a linear term in Q_a in the expansion (3.18), the pure vibrational contribution to the dipole polarizability is given by

$$\alpha_{ij}^{v}(-\omega;\omega) = \sum_a \frac{1}{\omega_a^2 - \omega^2} \frac{\partial \mu_i}{\partial Q_a} \frac{\partial \mu_j}{\partial Q_a}, \tag{3.19}$$

where the summation over all the normal modes include gradients of the dipole moment with respect to the normal coordinates Q_a. Expressions for vibrational contributions to the first and second hyperpolarizabilities β and γ at different approximation levels can be found in the literature [25].

Zero point vibrational averaging

Similarly as for the pure vibrational contribution we can now expand the electronic polarizability around the equilibrium geometry to estimate the effect of zero point vibrational averaging (ZPVA)

$$\alpha_{ij}(\mathbf{Q}) = \alpha_{ij}(\mathbf{0}) + \sum_a \frac{\partial \alpha_{ij}}{\partial Q_a} Q_a + \frac{1}{2} \sum_{a,b} \frac{\partial^2 \alpha_{ij}}{\partial Q_a \partial Q_b} Q_a Q_b + ... \tag{3.20}$$

For an anharmonic potential

$$V = V^0 + \frac{1}{2} \sum_a \omega_a^2 + \frac{1}{3!} \sum_{abc} F_{abc} Q_a Q_b Q_c + ... \tag{3.21}$$

we can write the zero point vibrationally averaged contribution as

$$\alpha_{ij}^{\Delta \mathrm{ZPVA}} = -\frac{1}{4} \sum_{ab} \frac{F_{abb}}{\omega_a^2 \omega_b} \frac{\partial \alpha_{ij}}{\partial Q_a} + \frac{1}{4} \sum_a \frac{1}{\omega_a} \frac{\partial^2 \alpha_{ij}}{\partial Q_a^2}. \tag{3.22}$$

The vibrational effects are usually more important for static properties than for dynamic properties. Nevertheless, there are cases when the vibrational contributions are non-negligible even for the dynamic properties. An example is two-photon absorption which will be discussed in chapter 5.

Chapter 4

Response theory

Expressions for molecular properties can be derived from standard time dependent perturbation theory using wave functions or density matrices (c.f. Eqs. (2.34)-(2.36)). The disadvantage of these so-called *sum-over-states* expressions is that they involve the calculation of the eigenstates of the unperturbed Hamiltonian, which also can be computationally very demanding. We are here primarily interested in a special class of molecular properties called non-linear optical properties. By calculating all the excited states we would receive much more information than we need - but we would also make more work than is necessary.

As indicated in the previous chapter, response theory [22] provides a very convenient, robust and general tool to overcome the difficulties with the summations over excited states. It is a formulation of time dependent perturbation theory in a general basis of orthonormal states in a way that makes it readily applicable for approximate wave functions. The wave function is parametrized in terms of exponential time dependent unitary operators and the time dependence if the parameters is determined by requiring Ehrenfests theorem to be satisfied in each order of the perturbation.

In practical calculations the straightforward approach would suffer by inverting very large matrices. However, an efficient algorithm involving only one-index contractions of such matrices and solving a set of linear equations makes it possible to apply response theory to the large molecules.

4.1 Response functions

Let us assume a perturbation to the Hamiltonian H in the form of a time-dependent operator V(t)

$$H = H_0 + V(t), \qquad V(t) = \int_{-\infty}^{\infty} V^{\omega} e^{(-i\omega+\epsilon)t} d\omega, \tag{4.1}$$

where a small real ϵ ensures that V(t) vanishes as we go $t \to -\infty$.

If the perturbation is sufficiently small we can write for the time development of a property A the following expansion

$$\begin{aligned}\langle A\rangle(t) &= \langle A\rangle_0 + \int_{-\infty}^{\infty}\langle\langle A;V^{\omega}\rangle\rangle e^{-i\omega t}d\omega \\ &+\frac{1}{2!}\int_{-\infty}^{\infty}\int_{-\infty}^{\infty}\langle\langle A;V^{\omega_1},V^{\omega_2}\rangle\rangle e^{-i(\omega_1+\omega_2)t}d\omega_1 d\omega_2 \\ &+\frac{1}{3!}\int_{-\infty}^{\infty}\int_{-\infty}^{\infty}\int_{-\infty}^{\infty}\langle\langle A;V^{\omega_1},V^{\omega_2},V^{\omega_3}\rangle\rangle e^{-i(\omega_1+\omega_2+\omega_3)t}d\omega_1 d\omega_2 d\omega_3 \\ &+\ldots,\end{aligned} \tag{4.2}$$

where $\langle\langle A, V^{\omega_1},...,V^{\omega_n}\rangle\rangle$ are the response functions. For the case of a property A being a dipole moment and a perturbation being an electric field the response functions would correspond to the polarizability and hyperpolarizabilities.

4.2 Response theory for an exact state

The time development of the exact wave function $|\overline{0}(t)\rangle$ is governed by the time dependent Schrödinger equation

$$H|\overline{0}(t)\rangle = i\frac{\partial}{\partial t}|\overline{0}(t)\rangle. \tag{4.3}$$

Assume that at the time $t \to -\infty$ the system was in the reference state $|0\rangle$ which is an eigenstate of H_0. We then parametrize the wave function in the following way

$$|\overline{0}(t)\rangle = e^{iF}|\tilde{0}(t)\rangle, \qquad |\tilde{0}(t)\rangle = \frac{|0\rangle + d_n|n\rangle}{\sqrt{1+\mathbf{d}^T\mathbf{d}}}, \tag{4.4}$$

where the phase factor F is a real function depending only on time, $\{|n\rangle\}$ is an orthonormal basis for the space orthogonal to $|0\rangle$ and the set of coefficients d_n describe the time development of the wave function. The denominator ensures normalization of the wave function.

It can be shown that for a state transfer operator $\tilde{R}_n = |\tilde{0}\rangle\langle\tilde{n}|$ *Ehrenfests theorem* holds

$$\frac{d}{dt}\langle\tilde{0}|\tilde{R}_n|\tilde{0}\rangle = \langle\tilde{0}|\frac{\partial}{\partial t}\tilde{R}_n|\tilde{0}\rangle - i\langle\tilde{0}|\left[\tilde{R}_n,H\right]|\tilde{0}\rangle. \tag{4.5}$$

This leads to the following equation for $\mathbf{d}$

$$\dot{\mathbf{d}} = -i\left(\mathbf{V}^{t[1]}\mathbf{E}^{[2]}\mathbf{d}\mathbf{V}^{t[2]}\mathbf{d} - \left(\mathbf{V}^{t[1]}\mathbf{d}\right)\mathbf{d}\right), \tag{4.6}$$

where we have introduced the matrix notation

$$V_n^{t[1]} = \langle n|V^t|0\rangle, \tag{4.7}$$
$$V_{nm}^{t[2]} = \langle n|V^t|m\rangle - \delta_{nm}\langle 0|V^t|0\rangle, \tag{4.8}$$
$$E_{nm}^{[2]} = \langle n|H_0|m\rangle - \delta_{nm}\langle 0|H_0|0\rangle. \tag{4.9}$$

After expanding $\mathbf{d}$ into a perturbation series we can derive the response functions as

$$\langle\langle V^{\omega_0}; V^{\omega_1}\rangle\rangle = -\sum_{\mathcal{P}} \mathbf{V}^{-\omega_0[1]^\dagger}\left(\mathbf{E}^{[2]} - \omega_1\mathbf{1}\right)^{-1}\mathbf{V}^{\omega_1[1]}, \tag{4.10}$$

$$\langle\langle V^{\omega_0}; V^{\omega_1}, V^{\omega_2}\rangle\rangle = \sum_{\mathcal{P}} \mathbf{V}^{-\omega_0[1]^\dagger}\left(\mathbf{E}^{[2]} - \omega_1\mathbf{1}\right)^{-1}\mathbf{V}^{\omega_1[2]}\left(\mathbf{E}^{[2]} - \omega_2\mathbf{1}\right)^{-1}\mathbf{V}^{\omega_2[1]}, \tag{4.11}$$

$$\begin{aligned}\langle\langle V^{\omega_0}; V^{\omega_1}, V^{\omega_2}, V^{\omega_3}\rangle\rangle = \sum_{\mathcal{P}} \Big\{ \Big[&-\mathbf{V}^{-\omega_0[1]^\dagger}\left(\mathbf{E}^{[2]} + \omega_0\mathbf{1}\right)^{-1}\mathbf{V}^{\omega_1[2]} \\ &\times \left(\mathbf{E}^{[2]} - (\omega_2+\omega_3)\,\mathbf{1}\right)^{-1}\mathbf{V}^{\omega_2[2]}\left(\mathbf{E}^{[2]} - \omega_3\mathbf{1}\right)^{-1}\mathbf{V}^{\omega_3[1]}\Big] \\ &+ \Big[\left(\mathbf{V}^{-\omega_0[1]^\dagger}\left(\mathbf{E}^{[2]} + \omega_0\mathbf{1}\right)^{-1}\left(\mathbf{E}^{[2]} - \omega_1\mathbf{1}\right)^{-1}\right) \\ &\times \left(\mathbf{V}^{-\omega_2[1]}\left(\mathbf{E}^{[2]} - \omega_3\mathbf{1}\right)^{-1}\mathbf{V}^{\omega_3[1]}\right)\Big]\Big\},\end{aligned} \tag{4.12}$$

where ω_0 is equal to $-\omega_1$, $-(\omega_1+\omega_2)$, and $-(\omega_1+\omega_2+\omega_3)$ for the first order, second order and the third order response functions, respectively.

If we choose the eigenstates of the unperturbed Hamiltonian as the basis we receive the so-called spectral representation of the response functions. For linear and quadratic response functions this representation looks as follows

$$\langle\langle V^{\omega_0}; V^{\omega_1}\rangle\rangle = -\sum_{\mathcal{P}} \frac{\langle 0|V^{\omega_0}|n\rangle\langle n|V^{\omega_1}|0\rangle}{\omega_n - \omega_1}, \tag{4.13}$$

$$\langle\langle V^{\omega_0}; V^{\omega_1}, V^{\omega_2}\rangle\rangle = \sum_{\mathcal{P}} \frac{\langle 0|V^{\omega_0}|n\rangle\langle n|\left(V^{\omega_1} - \langle 0|V^{\omega_1}|0\rangle\right)|m\rangle\langle m|V^{\omega_2}|0\rangle}{(\omega_n+\omega_0)(\omega_m-\omega_2)}. \tag{4.14}$$

4.3 Molecular properties from response functions

4.3.1 Non-resonant properties

Setting the property operator to the dipole moment operator we can directly relate the linear response function with the polarizability α, the quadratic response function with the first hyperpolarizability β and the cubic response function with the second hyperpolarizability γ. In the spectral representation, where the eigenstates of the

unperturbed Hamiltonian are the basis for the expansion, we get

$$\alpha_{ij}(-\omega_\sigma;\omega_1) = -\langle\langle \mu_i;\mu_j\rangle\rangle_{\omega_1} = \sum_{n\neq 0}\left[\frac{\langle 0|\mu_i|n\rangle\langle n|\mu_j|0\rangle}{\omega_n-\omega_1}+\frac{\langle 0|\mu_j|n\rangle\langle n|\mu_i|0\rangle}{\omega_n+\omega_1}\right], \quad (4.15)$$

$$\beta_{ijk}(-\omega_\sigma;\omega_1,\omega_2) = \sum_{\mathcal{P}}\sum_{n,m\neq 0}\frac{\langle 0|\mu_i|n\rangle\langle n|\tilde{\mu}_j|m\rangle\langle m|\mu_k|0\rangle}{(\omega_n-\omega_\sigma)(\omega_m-\omega_2)}, \quad (4.16)$$

$$\gamma_{ijkl}(-\omega_\sigma;\omega_1,\omega_2,\omega_3) = \sum_{\mathcal{P}}\left[\sum_{n,m,o\neq 0}\frac{\langle 0|\mu_i|n\rangle\langle n|\tilde{\mu}_j|m\rangle\langle m|\tilde{\mu}_k|o\rangle\langle o|\mu_l|0\rangle}{(\omega_n-\omega_\sigma)(\omega_m-\omega_2-\omega_3)(\omega_o-\omega_2)}\right.$$

$$\left.+\sum_{n,m\neq 0}\frac{\langle 0|\mu_i|n\rangle\langle n|\mu_j|0\rangle\langle 0|\mu_k|m\rangle\langle m|\mu_l|0\rangle}{(\omega_n-\omega_\sigma)(\omega_n-\omega_1)(\omega_m+\omega_2)}\right], \quad (4.17)$$

where $\tilde{\mu}_j$ is the fluctuating dipole moment $\mu_j - \langle 0|\mu_j|0\rangle$, ω_σ is the sum of frequencies of the perturbing fields; $\omega_\sigma = \omega_1+\omega_2+...\omega_n$ and $\sum_{\mathcal{P}}$ denotes a summation over simultaneous permutations of the operators and their corresponding frequencies. These equations are the non-resonant limits of the equations (2.34)-(2.36).

4.3.2 Excitation energies and residues

From the spectral representation of the linear response function (4.13) we see that it has poles at the frequencies equal to the excitation energies. In the general basis the linear response function (4.10) has poles when the matrix $\left(\mathbf{E}^{[2]}-\omega_1\mathbf{1}\right)$ is singular. In other words, we have to solve the eigenvalue problem

$$\mathbf{E}^{[2]}X^{\mathrm{f}} = \omega_f X^{\mathrm{f}}. \quad (4.18)$$

The residue corresponding to the pole $\omega_1 = \omega_f$ is

$$\lim_{\omega_1\to\omega_f}(\omega_1-\omega_f)\,\langle\langle \mu_i;\mu_j\rangle\rangle_{\omega_1} = \langle 0|\mu_i|f\rangle\langle f|\mu_j|0\rangle, \quad (4.19)$$

thus providing us the tool to obtain the oscillator strength (or absolute value of the transition moment) of the transition from the ground electronic state $|0\rangle$ to the final electronic state $|f\rangle$. Similarly, the single residue of the quadratic response function [22] can be used to identify the two-photon transition matrix element (5.7) as

$$\lim_{\omega\to\omega_f}(\omega_f-\omega)\langle\langle \mu_i;\mu_j,\mu_k\rangle\rangle_{\frac{1}{2}\omega_f,\omega} = S_{ij}\langle f|\mu_k|0\rangle. \quad (4.20)$$

4.4 Response theory for an SCF reference state

The closed shell Hartree-Fock state can be parametrized in the following exponential way

$$|\tilde{0}_{HF}\rangle = e^{i\hat{\kappa}}|0_{HF}\rangle, \quad (4.21)$$

where $\hat{\kappa}$ is a Hermitian operator defined as

$$\hat{\kappa} = \sum_{pq} \kappa_{pq} E_{pq}, \qquad E_{pq} = a^\dagger_{p\alpha} a_{q\alpha} a^\dagger_{p\beta} a_{q\beta}, \tag{4.22}$$

and where E_{pq} is an orbital rotation generator and $a^\dagger, a$ are electron creation and annihilation operators. We will denote by a, b virtual, by i, j, k, l occupied, by p, q, r, s general molecular orbitals and by $\mu, \nu, \delta, \lambda$ atomic orbitals. We introduce a more general operator basis $\mathbf{O}$ with the structure $\mathbf{O} = \left(\mathbf{q}^\dagger, \mathbf{q}\right) \mathbf{X}$ as the transformation of the excitation and de-excitation operators $q^\dagger = E_{ai}, q = E_{ia}$. The operator $\boldsymbol{\kappa}$ can be written in this general basis as

$$\boldsymbol{\kappa} = \mathbf{O}\boldsymbol{\alpha}, \qquad \boldsymbol{\alpha} = \mathbf{X}^{-1} \begin{pmatrix} \boldsymbol{\kappa} \\ \boldsymbol{\kappa}^* \end{pmatrix}. \tag{4.23}$$

The time development of the SCF state can be now be determined from the set of Ehrenfests equations

$$\frac{d}{dt} \langle \tilde{0}(t) | \tilde{\boldsymbol{O}}^\dagger | \tilde{0}(t) \rangle = \langle \tilde{0}(t) | \dot{\tilde{\boldsymbol{O}}}^\dagger | \tilde{0}(t) \rangle - i \langle \tilde{0}(t) | \left[\tilde{\boldsymbol{O}}^\dagger, H_0 + V^t \right] | \tilde{0}(t) \rangle, \tag{4.24}$$

with the operator basis $\tilde{O}_i = e^{i\kappa} O_i e^{-i\kappa}$.

By solving these equations to the first order of perturbation we can obtain the linear response function in the elementary basis

$$\langle\langle A; B \rangle\rangle_{\omega_1} = -\mathbf{A}^{[1]} \left(\mathbf{E}^{[2]} - \omega_1 \mathbf{S}^{[2]} \right)^{-1} \mathbf{B}^{[1]}, \tag{4.25}$$

where the matrices $\mathbf{E}^{[2]}$ and $\mathbf{S}^{[2]}$ are defined

$$A^{[1]}_n = \langle 0 | [O^\dagger_n, A] | 0 \rangle, \tag{4.26}$$
$$S^{[2]}_{nm} = \langle 0 | [O^\dagger_n, O_m] | 0 \rangle, \tag{4.27}$$
$$E^{[2]}_{nm} = -\langle 0 | [O^\dagger_n, [O_m, H_0]] | 0 \rangle. \tag{4.28}$$

This expression involves inverting $\mathbf{E}^{[2]} - \omega_1 \mathbf{S}^{[2]}$ which is typically a large matrix of the size of the order of $10^4 - 10^5$. To avoid this we can utilize the fact that we need to evaluate only the product of this inversed matrix with the vector $\mathbf{B}^{[1]}$. Hence we can instead solve the linear equation

$$\left(\mathbf{E}^{[2]} - \omega_1 \mathbf{S}^{[2]} \right) \mathbf{N}^B(\omega_1) = \mathbf{B}^{[1]}. \tag{4.29}$$

A contraction of the $\mathbf{E}^{[2]}$ and $\mathbf{S}^{[2]}$ matrices is much easier to perform directly. Thus using such a direct method we never need to construct these large matrices explicitly. This makes it possible to make linear response calculations at the costs comparable to the cost of the wave function calculation itself.

Similarly, the quadratic response function can be expressed as

$$\begin{aligned}\langle\langle A;B,C\rangle\rangle_{\omega_1,\omega_2} &= \mathbf{N}_n^A(\omega_1+\omega_2)\mathbf{B}_{nm}^{[2]}\mathbf{N}_m^C(\omega_2)+\mathbf{N}_n^A(\omega_1+\omega_2)\mathbf{C}_{nm}^{[2]}\mathbf{N}_m^B(\omega_1) \\ &+ \mathbf{N}_n^B(\omega_1)\left(\mathbf{A}_{nm}^{[2]}+\mathbf{A}_{mn}^{[2]}\right)\mathbf{N}_m^C(\omega_2) \\ &- \mathbf{N}_n^A(\omega_1+\omega_2)\left(\mathbf{E}_{nmo}^{[3]}+\mathbf{E}_{nom}^{[3]}-\omega_1\mathbf{S}_{nmo}^{[3]}-\omega_2\mathbf{S}_{nom}^{[3]}\right)\mathbf{N}_m^B(\omega_1)\mathbf{N}_o^C(\omega_2),\end{aligned} \tag{4.30}$$

where

$$A_{nm}^{[2]} = \langle 0|[O_n^\dagger, A]|0\rangle, \tag{4.31}$$

$$S_{nmo}^{[3]} = \langle 0|[O_m^\dagger,[O_n,O_o]]|0\rangle, \tag{4.32}$$

$$E_{nmo}^{[3]} = -\langle 0|[O_m^\dagger,[O_n,[O_o,H_0]]]|0\rangle. \tag{4.33}$$

From the linear response function we see that the excitation energy is obtained by solving the generalized eigenvalue equation

$$\left(\mathbf{E}^{[2]}-\omega_f\mathbf{S}^{[2]}\right)X^{\mathrm{f}}=0. \tag{4.34}$$

For the two-photon transition moment (4.20) we obtain

$$\begin{aligned}S_{AB} &= -N_n^A(\omega_f/2)B_{nm}^{[2]}N_m^F(\omega_f)-N_n^B(-\omega_f/2)A_{(nm)}^{[2]}N_m^F(\omega_f) \\ &- N_n^A(\omega_f/2)\left(E_{n(mo)}^{[3]}+\frac{1}{2}\omega_f S_{nmo}^{[3]}-\omega_f S_{nmo}^{[3]}\right)N_m^B(-\omega_f/2)N_o^F(\omega_f),\end{aligned} \tag{4.35}$$

$$N_n^X(\omega) = \left(E^{[2]}-\omega S^{[2]}\right)^{-1}_{nm}X_m^{[1]}, \qquad X\in\{A,B\}, \tag{4.36}$$

$$0 = \left(E^{[2]}-\omega_f S^{[2]}\right)^{-1}_{nm}N_m^F. \tag{4.37}$$

4.5 Excited state gradient

The excited state properties can be obtained as the higher order residues of the response functions. An alternative approach is to set up an excited state Lagrangian and calculate the analytical derivatives from it. An example of such a calculation can be the gradient of the excited state energy.

Considering the normalized eigenvectors from Eq. (4.34) we can write the excitation energy as

$$E^f = E^0+\omega^f, \qquad \omega^f = {\mathbf{X}^{\mathrm{f}}}^\dagger{}_n E_{nm}^{[2]}\mathbf{X}_m^{\mathrm{f}}. \tag{4.38}$$

A Lagrangian can be constructed for the excited state energy with the normalization and variational constrains [24]

$$L^f = E^0+{X^{\mathrm{f}}}^\dagger{}_n E_{nm}^{[2]}X_m^{\mathrm{f}}+\overline{\alpha}\left({X^{\mathrm{f}}}^\dagger{}_n S_{nm}^{[2]}X_m^{\mathrm{f}}-1\right)+\overline{\kappa}_n^f\frac{\partial E}{\partial\kappa_n}, \tag{4.39}$$

where $\overline{\alpha}$ and $\overline{\kappa}^f$ are Lagrange multipliers. We require the Lagrangian to be variational in all parameters $\kappa, \overline{\kappa}, \overline{\alpha}, X^{\mathrm{f}}$ and $X^{\mathrm{f}\dagger}$. Using the variational constraints for these parameters we can obtain for the excited state gradient

$$\frac{dL^f}{dx} = \frac{dE^o}{dx} + X^{\mathrm{f}\dagger}{}_n \frac{\partial E^{[2]}_{nm}}{\partial x} X^{\mathrm{f}}_m + \overline{\kappa}^f_n \frac{\partial^2 E}{\partial \kappa_n \partial x}, \tag{4.40}$$

where the lagrange multiplier $\overline{\kappa}^f$ is determined from the equation

$$E^{[2]}_{nm} \overline{\kappa}^f_m = X^{\mathrm{f}}_m \frac{\partial E^{[2]}_{mo}}{\partial \kappa_n} X^{\mathrm{f}}_o. \tag{4.41}$$

In order to be able to make applications for large molecules we need to express everything in a direct fashion and in the atomic orbital basis. The basis set dependence also requires that we use so-called orthonormalized molecular orbitals [26].

4.6 Response theory beyond the random phase approximation

There are two approximations involved in response theory for approximate wave functions - the reference wave function and the parametrization of the time development of this reference wave function.

We have shown the case of the SCF reference wave function. Another example, treating correlation, is the MCSCF reference wave function, which can be parametrized as

$$|\tilde{0}\rangle = e^{i\hat{\kappa}} e^{i\hat{S}} |0\rangle, \tag{4.42}$$

where $\hat{S}$ describes the variations in the configuration space

$$\hat{S} = S_n R^\dagger_n + S^*_n R_n, \tag{4.43}$$

with R_n being a state transfer operator. Solving the Ehrenfests equations for the general operator basis gives the response functions for MCSCF wave functions.

We can include also double excitations and deexcitatons in the particle-hole excitation operator manifold, leading to the second order polarization propagator approach (SOPPA) and higher order propagator approaches [27, 28].

Chapter 5

Two-photon absorption

If the frequency of the light is close to a resonant frequency in the molecule (excitation energy) an absorption of a photon may occur. The probability of absorbing a photon depends linearly on the light intensity in this case. If the sum of the frequencies of two light beams is close to a resonant frequency of a molecule a simultaneous absorption of two photons may occur. The two-photon absorption process is also possible from a strong single beam when the frequency is half of the excitation energy. In contrast to the case of one-photon absorption the probability of absorbing two photons depends quadratically on the light intensity.

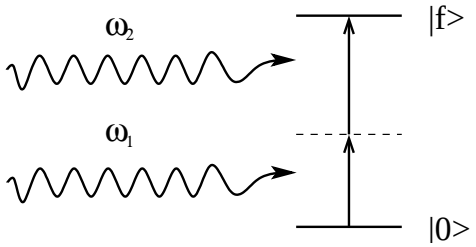

Figure 5.1: Schematic picture of the Two-Photon Absorption (TPA). Strong incoming field at frequencies ω_1, ω_2 can result in absorption of two-photon quanta and excite the molecule to a level with the energy $\omega_1 + \omega_2$ above the ground state.

The two-photon absorption process we describe here is an instantaneous coherent absorption of two photon quanta. Since the single frequencies ω_1 or ω_2 do not match any resonance[1] it is a very fast process on the femtosecond time scale[2].

The main features of the two-photon absorption process are the following

- There are **different selection rules** compared to one-photon absorption. For example, in the system with inversion symmetry only g-g and u-u transitions are two-photon allowed.

[1] In the resonant case it would be two-step process, usually occurring in so-called a pump-probe experiments.

[2] The time of the process is related to the detuning of the frequencies from resonances.

- It shows special **dependence on the polarization** of the light and different cross section for circularly polarized light than for linearly polarized. In contrast to one-photon absorption the cross section is dependent on the light polarization even for randomly oriented molecules.
- It has **quadratic dependence on the intensity** of the incoming light.
- A **low frequency of the light** is sufficient for excitation.

The two-photon absorption process was theoretically predicted by Göppert-Mayer already in 1931 [3], but the first experimental observations came in 1961 after the invention of the laser [4]. In the early days of two-photon absorption it was mostly used for spectroscopic purposes. Due to different selection rules and dependence of the TPA cross section on the polarization of light even for randomly oriented species (in relation with the symmetry of the excited state) it became a valuable tool for investigating the excited states unaccessible for one-photon spectroscopy. The so-called Doppler free two-photon spectroscopy using two differently circularly polarized beams was able to overcome major broadenings in the spectra of gas phase molecules. However, nowadays the two-photon absorption has turned out to be very attractive for many practical applications. The main advantages of TPA for these applications are the quadratic dependence of the TPA and the lower frequency required for excitation. These features can be utilized in various applications [29]:

- **Optical power limiting.** Two-photon absorption connected with the excited state absorption is a good mechanism for fast optical limiting devices.
- **3D optical data storage.** The advantage of using TPA in this area would be its potential for fast reading and writing potential, the random access and the potentially low cost.
- **Two-photon pumped upconverted lasing.** The desire for low cost solid state blue lasers for data storage and optical communication has motivated an examination of two-photon absorption for upconversion. The two-photon absorption process has the advantage of not requiring a phase-matching condition for the upconversion.
- **Two-photon laser scanning confocal microscopy.** The possibility of using light at larger wavelengths (near IR region) has the advantage of reducing the damage of the sample.
- **Two-photon photodynamic cancer therapy.** The usual photodynamic cancer therapy is based on photo-excitation with visible light of the photosensitizer concentrated in the malignant tumor cells. This results in the release of singlet oxygen acting destructively on cancerous cells. The main problem is the poor penetrability of the living tissue in the visible range. Two-photon absorption

would utilize the light at longer wavelengths which has much better penetration in living tissue.

All of these applications require molecules with a sufficiently large TPA cross section. Organic molecules are very good candidates in the search for high TPA cross sections, because their large flexibility makes them suitable for optimizing the property of interest. For example, different donor and acceptor substituted π-conjugated systems have been found to be good candidates as discussed in this thesis.

It is usually difficult to compare the absolute TPA cross sections of different materials based on an evaluation of available experimental results. This is either because the measurements by different groups were not always carried out under comparable experimental conditions, or because that some of the materials were only measured using one single wavelength [30, 31]. Theoretical simulations, on the other hand, should be able to provide a fair comparison among different TPA materials under conditions that are appropriate for comparison.

5.1 Two-photon absorption cross sections

We have shown in section 2.1.4 that two-photon absorption is connected with the imaginary part of the third order susceptibility $\chi^{(3)}(-\omega_1; -\omega_1, \omega_2, -\omega_2)$. For simplicity we shall consider the case of one beam with frequency ω being close to half of the excitation energy of the final state ω_f. Recalling the expression for the averaged amount of absorbed power (2.12) and that the intensity is $I = \frac{1}{2}\epsilon_0 c E^2$ (in SI units)

$$\left\langle \frac{d}{dt}\left(\frac{\text{absorbed energy}}{\text{volume}}\right)\right\rangle = \frac{\omega}{4\epsilon_0^2 c^2} Im\left[\chi^{(3)}\right] I^2. \tag{5.1}$$

In the nonlinear transition experiment, the two-photon absorption cross section is defined as (see e.g. [10])

$$\sigma^{(2)} = \frac{\hbar\omega}{N}\alpha^{(2)}, \tag{5.2}$$

where N is the density of the molecules and $\alpha^{(2)}$ is the two-photon absorption coefficient describing the quadratic term in the attenuation of the beam intensity

$$\frac{dI}{dz} = -\alpha^{(1)} I - \alpha^{(2)} I^2. \tag{5.3}$$

For randomly oriented samples we need to consider the orientationally averaged two-photon absorption cross section σ_{TP} which is given by

$$\sigma_{TP} = \frac{4\pi^3 a_0^5 \alpha}{15c}\omega^2 \Delta\left(\omega_f - 2\omega, \Gamma_f\right)\delta_{TP}. \tag{5.4}$$

The resulting units are cm^4 sec photon^{-1}, provided that the Bohr radius a_0 and speed of light c are given in the SI units and the frequency of the light ω, broadening of the final state Γ_f and the orientationally averaged two-photon probability δ_{TP} are given in atomic units (α is the fine structure constant). The normalized Lorenzian $\Delta(\omega_f - 2\omega, \Gamma_f)$ in the expression is

$$\Delta(\omega_f - 2\omega, \Gamma_f) = \frac{1}{\pi} \frac{\Gamma_f}{(\omega_f - 2\omega)^2 + \Gamma_f^2}. \tag{5.5}$$

The orientationally averaged two-photon probability δ_{TP} is given by [32]

$$\delta_{TP} = \sum_{ij} \left[F \times S_{ij} S_{ji}^* + G \times S_{ij} S_{ij}^* + H \times S_{ij} S_{ji}^* \right], \tag{5.6}$$

Here F, G and H are coefficients dependent on the polarization of the light and S_{ij} is the two-photon transition matrix element

$$S_{ij} = \sum_k \left[\frac{\langle 0|\mu_i|k\rangle\langle k|\mu_j|k\rangle}{\omega_k - \omega} + \frac{\langle 0|\mu_j|k\rangle\langle k|\mu_i|k\rangle}{\omega_k - \omega} \right], \tag{5.7}$$

where the summation runs over all the intermediate states $|k\rangle$. For two photons from the same beam the S matrix is symmetrical and the coefficients F, H and G are 2, 2 and 2 for a linearly polarized light beam and -2, 3 and 3 for a circularly polarized beam, respectively.

We can see, that unlike one-photon absorption which gives the same orientationally averaged cross section for linearly and circularly polarized light, the two-photon absorption is dependent on the polarization of the light. If the S matrix is dominated by one diagonal element, for example S_{xx}, then the two-photon absorption probability reduces to

$$\delta_{TP} = [F + G + H] S_{xx} S_{xx}^*, \tag{5.8}$$

which considering the values of coefficients of F, G and H, would give a ratio $\delta_{TP}^{lin}/\delta_{TP}^{cir}$ equal to 1.5. On the other hand, for the traceless S matrix Eq. (5.6) turns to

$$\delta_{TP} = G \times \sum_{ij} S_{ij} S_{ij}^* + H \times \sum_{ij} S_{ij} S_{ji}^*. \tag{5.9}$$

Taking again into account the values of G and H coefficients for linearly and circularly polarized light we obtain the ratios of $\delta_{TP}^{lin}/\ \delta_{TP}^{cir}$ to be equal to 0.67.

5.2 Vibrational contributions

Including summation over vibronic states explicitly the first part of the TPA transition moment gives

$$S_{ij} = \sum_{K,k} \frac{\langle 0,0|\mu_i|K,k\rangle\langle K,k|\mu_j|F,f\rangle}{\omega_K + \omega_k - \omega} + \sum_{K,k} \frac{\langle 0,0|\mu_j|K,k\rangle\langle K,k|\mu_i|F,f\rangle}{\omega_K + \omega_k - \omega}, \qquad (5.10)$$

where the summation goes over all intermediate electronic and vibrational states and where $|F\rangle$ and $|f\rangle$ specify the final electronic and vibrational states, respectively.

We can assume that, similar to the case of the polarizability, $\omega_K - \omega >> \omega_f$, so ω_f in the denominator can be neglected. Then, using the closure formula, we get for the first term in (5.10)

$$S_{ij} \quad = \quad \langle 0^{\mathrm{v}}|S^E_{ij}(\mathbf{Q})|f\rangle, \qquad (5.11)$$

where $S^E_{ij}(\mathbf{Q})$ is the electronic part of the TPA matrix element dependent on the nuclear geometry

$$S^E_{ij}(\mathbf{Q}) \quad = \quad \sum_n \left[\frac{\langle 0|\mu_i|K\rangle\langle K|\mu_j|F\rangle}{\omega_K - \omega} + \frac{\langle 0|\mu_j|K\rangle\langle K|\mu_i|F\rangle}{\omega_K - \omega} \right]. \qquad (5.12)$$

Expanding $S^E_{ij}(\mathbf{Q})$ in the normal modes we have

$$S^E_{ij}(\mathbf{Q}) = S^E_{ij}(\mathbf{Q}) + \sum_a \frac{\partial S^E_{ij}}{\partial Q_a} Q_a + \ldots \qquad (5.13)$$

which for the total TPA transition moment means

$$S_{ij} \quad = \quad S^E_{ij}(\mathbf{0})\langle 0^{\mathrm{v}}|f\rangle + \sum_a \frac{\partial S^E_{ij}}{\partial Q_a}\langle 0^{\mathrm{v}}|Q_a|f\rangle. \qquad (5.14)$$

Here the first term contains an ordinary Franc-Condon factor and the second term the Herzberg-Teller type contributions to the two-photon absorption. In this thesis we use two different approximations for the excited state potential surfaces.

5.2.1 Zero-order harmonic approximation

If we approximate also the excited state (harmonic) potential surface by the ground state (harmonic) potential surface we receive

$$S_{ij} \quad = \quad S^E_{ij}(\mathbf{0}) \prod_a \delta_{0n^f_a} + \frac{1}{\sqrt{2\omega_a}} \frac{\partial S^E_{ij}}{\partial Q_a} \delta_{0n^f_a} \prod_{b \neq a} \delta_{0n^f_b} \qquad (5.15)$$

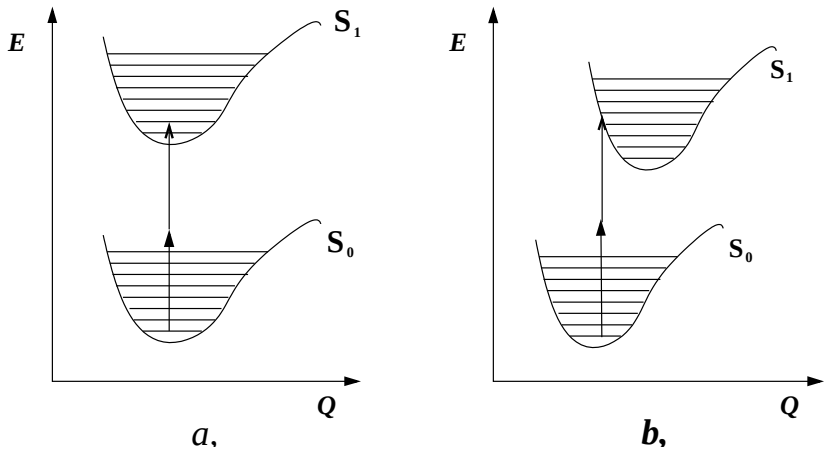

Figure 5.2: Two models for the ground and excited state potential surface: (a) parallel harmonic potential surfaces; (b) displaced harmonic potential surfaces with the same curvature (linear coupling model).

where n_a^f denotes the occupation number of the final vibrational state $|f\rangle$ in the normal mode a. The meaning of this formula is simply that apart from the 0-0 transition only transitions to such final vibrational states in which one normal mode is singly excited may occur.

5.2.2 Linear coupling model

We consider the situation when the excited state potential surface is approximated by the ground state harmonic potential surface with the same curvature but displaced along the normal coordinates. The displacement d_a of the normal mode a in the excited state potential surface is connected to the gradient G_a of the excited state energy

$$d_a = \frac{G_a}{\omega_a^2}, \qquad G_a = \frac{\partial E^{S_1}}{\partial Q_a}, \tag{5.16}$$

A general expression for the overlap between two displaced vibronic states for one normal mode a with occupation numbers $m_a > n_a$ can be written as

$$\langle m_a | n_a \rangle = e^{-\frac{x}{2}} x^{\frac{m_a - n_a}{2}} \sqrt{\frac{n_a!}{m_a!}} L_{n_a}^{m_a - n_a}(x), \tag{5.17}$$

where x is a dimensionless parameter dependent on the displacement d and frequency of the normal mode as $x = \frac{\omega_a d_a^2}{2\hbar}$, and $L_{n_a}^{m_a - n_a}(x)$ is the associated Laguerre

polynomial;

$$L_{n_a}^{m_a-n_a}(x) = \sum_{r=0}^{n_a} \frac{m_a!(-x)^r}{(n_a-r)!(m_a-n_a+r)!r!}. \tag{5.18}$$

For $m_a < n_a$ we have $\langle m_a|n_a\rangle = (-1)^{n_a-m_a}\langle n_a|m_a\rangle$.

The matrix elements between two vibrational wave functions of the same harmonic oscillator (normal mode) a are

$$\langle 0^0|n_a^F\rangle = e^{-\frac{x}{2}}(-1)^{n_a^F}\frac{x^{\frac{n_a^F}{2}}}{\sqrt{n_a^F!}}, \tag{5.19}$$

$$\langle 0^0|Q_a|n_a^F\rangle = \sqrt{\frac{\hbar}{2\omega_a}}e^{-\frac{x}{2}}\frac{(-1)^{n_a^F}x^{\frac{n_a^F-1}{2}}}{\sqrt{n_a^F!}}\left(x-n_a^F\right), \tag{5.20}$$

where n_a is the occupation number. For a multimode situation we have

$$\langle 0^0|f^F\rangle = \prod_a \langle m_a^0|n_a^F\rangle, \tag{5.21}$$

$$\langle 0^0|Q_a|f^F\rangle = \langle m^0|Q_a|n_a^F\rangle \prod_{b\neq a}\langle m_b^0|n_b^F\rangle. \tag{5.22}$$

5.2.3 Sum rules

By summing over all the final vibrational states one gets

$$\sum_{f^F} S_{\alpha\alpha}S_{\beta\beta}^* = \sum_{f^F}\Bigg[\langle 0^0|S_{\alpha\alpha}^e(Q_{eq}) + \sum_a \frac{\partial S_{\alpha\alpha}^e}{\partial Q_a}Q_a|f^F\rangle\,, \tag{5.23}$$

$$\langle f^F|S_{\beta\beta}^{e\,*}(Q_{eq}) + \sum_b \frac{\partial S_{\beta\beta}^{e\,*}}{\partial Q_b}Q_b|0^0\rangle\Bigg]. \tag{5.24}$$

The sum over all final vibrational modes in the final electronic state F then results in

$$\delta_{TP}^F = \sum_{f^F}\delta_{TP} = 2\sum_{\alpha\beta}\left[S_{\alpha\alpha}S_{\beta\beta}^* + S_{\alpha\beta}S_{\alpha\beta}^* + S_{\alpha\beta}S_{\beta\alpha}^*\right] \tag{5.25}$$

$$+ \quad 2\sum_a\sum_{\alpha\beta}\frac{1}{2\omega_a}\left[\frac{\partial S_{\alpha\alpha}^e}{\partial Q_a}\frac{\partial S_{\beta\beta}^{e\,*}}{\partial Q_a} + \frac{\partial S_{\alpha\beta}^e}{\partial Q_a}\frac{\partial S_{\alpha\beta}^{e\,*}}{\partial Q_a} + \frac{\partial S_{\alpha\beta}^e}{\partial Q_a}\frac{\partial S_{\beta\alpha}^{e\,*}}{\partial Q_a}\right]. \tag{5.26}$$

Thus the overall Herzberg-Teller contribution to the two-photon absorption depends only on the TP transition moment gradient, but not on the excited state potential surface.

5.3 One dimensional molecules

The most efficient TPA materials seem to be the ones with various electron-donor (D) and electron-acceptor (A) groups attached symmetrically or asymmetrically to a conjugated linker (π-center). In this thesis, we have theoretically examined a series of organic molecules (see paper IX) that exhibit large two-photon absorption cross sections in the visible region and that have been synthesized in different laboratories [33, 30, 34, 35, 31], see Fig. 5.3. Three different π-centers, namely dithienothiophene (DTT), trans-stilbene and fluorene, have been used in these compounds.

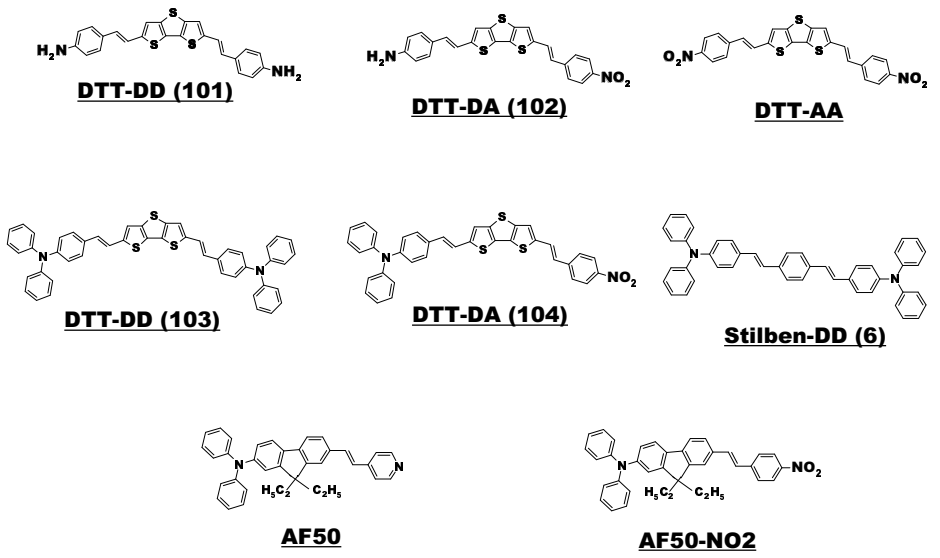

Figure 5.3: Structures of some one-dimensional TPA molecules.

We examined several factors that determine strong TPA cross section in these compounds. The molecular length seems to be the most important parameter for determining the one-photon absorption (OPA) intensities of active TPA materials. AF50 has quite small oscillator strength, probably due to its small size. With its stronger acceptor strength AF50-NO2 shows slightly larger oscillator strength, but still much smaller than all the DTT compounds we have considered, indicating that the choice of donor, acceptor and π-center has small impact on the OPA. However, the substitu-

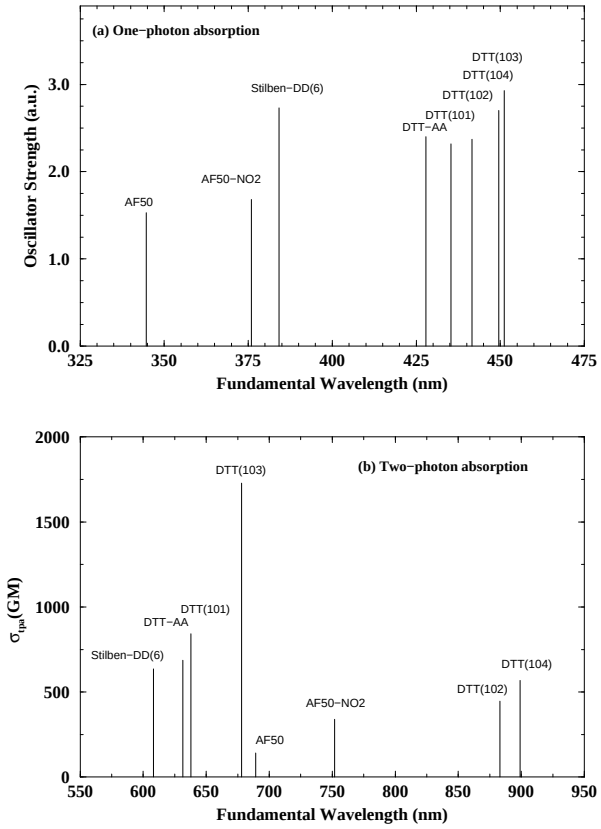

Figure 5.4: Maximum one-, and two-photon absorption cross sections of some studied molecules. 1GM=10^{-50} cm^4 photon^{-1} s.

tion and the symmetry a of molecule has strong impact on the TPA cross section. For a given π-center, the use of a stronger donor or acceptor has very positive effects on the TPA cross section, while still the most important role is played by the molecular symmetry; as shown in Fig. 5.4, the two D/D paired molecules have the largest TPA cross sections. Our calculated results have thus confirmed the experimental findings on the importance of the molecular symmetry [36]. It clearly shows in Fig. 5.4 that DTT-DD(103) has an outstanding TPA activity. The DTT-DD(101), DTT-AA, Stilben-DD(6) and DTT-DA(104) compounds belong to the same group with very attractive TPA properties.

5.4 Few state models

The transition dipole moments and dipole moment changes in the lowest excited states of the charge transfer molecules are so large, that the TPA cross section can be approximated by including only few states in the summation. Response theory provides an analytical solution for computing the TPA cross sections, in which all excited states involved in the process are taken into account, and can thus serve as reference for examining reliability of such few state models.

The TPA cross section of one-dimensional molecules is completely dominated by the component along the molecular axis S_{zz}, and only this component will be considered in a few state model. For the symmetrically substituted one-dimensional molecules, the first excited state is two-photon forbidden. Thus we have to use at least a three state model for calculation of the TPA cross section

$$S_{zz}^{TP} = \frac{2{\mu_z}^{01}{\mu_z}^{1f}}{\Delta E}, \qquad \Delta E = \omega_1 - \omega = \omega_1 - \frac{\omega_f}{2}. \tag{5.27}$$

For asymmetrically substituted molecules it is sufficient to include only two states

$$S_{zz}^{TP} = \frac{2{\mu_z}^{0f}\left(\mu_z^{ff} - \mu_z^{00}\right)}{\Delta E}, \qquad \Delta E = \hbar\omega_f - \omega = \frac{\omega_f}{2}. \tag{5.28}$$

The two and three state models for asymmetrically and symmetrically substituted molecules, respectively, compare very well with the full response calculation results (see Tab. 5.1).

Molecule	ΔE (eV)	${\mu_z}^{0f}$ (D)	$\Delta\mu_z$ (D)	S_{zz} (2 st)	S_{zz} (resp.)	σ_{tpa} (2 st.)	σ_{tpa} (resp.)
DTT-DA(102)	1.66	13.6	4.5	309	293	498	446
DTT-DA(104)	1.63	14.6	4.7	355	334	645	568
Molecule	ΔE (eV)	${\mu_z}^{01}$ (D)	${\mu_z}^{1f}$ (D)	S_{zz}(3 st.)	S_{zz} (resp.)	σ_{tpa} (3 st.)	σ_{tpa} (resp.)
DTT-AA	1.19	13.5	2.5	243	273	541	687
Stilbene-DD (6)	1.44	13.7	3.1	246	258	613	636
DTT-DD (101)	1.15	13.4	2.9	286	302	755	842
DTT-DD (103)	1.17	15.3	4.0	441	461	1594	1727

Table 5.1: Comparison of the few state models with response calculations for strong charge transfer one-dimesional donor/acceptor substituted molecules.

Few state models are also very useful for explanation of the results and for qualitative analyses of the observed trends. The transition moments and energies used in the three state model for four symmetrically substituted molecules are illustrated in Fig. 5.5. It is quite clear that the DTT-DD(103) molecule should have the largest TPA cross section because it possesses the largest transition moments μ_z^{01}, μ_z^{12} and one of the smallest energy differences, ΔE among all these molecules.

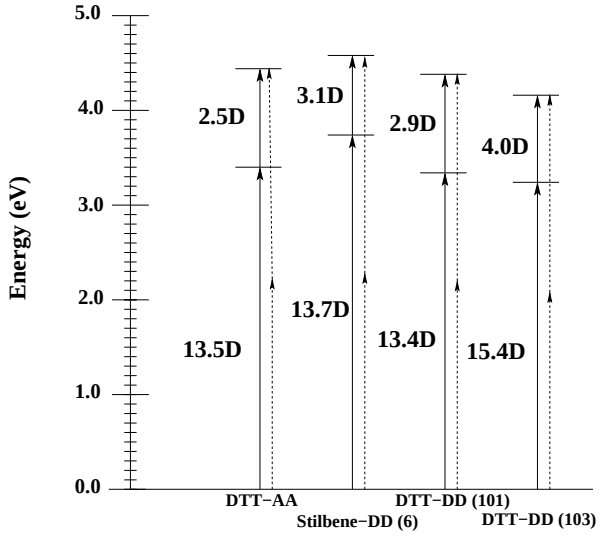

Figure 5.5: Transition moments and excitation energies used in the few state model for molecules with high two-photon absorption cross sections.

5.5 Multi-branched molecules

An electron-rich π-center attached to symmetrically substituted donors constitutes an optimal one-dimensional structure for maximizing the TPA cross sections in the visible region, as demonstrated by the DTT-DD(103) compound. It was shown that the TPA cross section can also be enhanced efficiently by increasing the dimensionality of the π center [37], which in a way is equivalent to increasing the strength of the π center. A two-dimensional CT system based on 1,2-di(9H-9-fluorenylidene) ethene has shown a very large TPA cross section, taking a value as high as 1732 (GM), which is quite comparable to the DTT-DD(103) compound. This observation seems to be consistent with experimental measurements on some multi-branched structures [38], denoted as PRL-101, PRL-501 and PRL-701, in which it was found that such structures significantly increase the TPA cross section compared with the one-branched counterparts. Such an enhancement was ascribed the electronic coupling between different branches. We have calculated the TPA cross sections of PRL-101 and PRL-501 at the RPA level with 6-31G basis set (paper VI) and found that there is no strong enhancement of the TPA cross sections going from PRL-101 to PRL-501. As a matter of fact, the TPA of the first CT state of PRL-501 is about half the value of that for PRL-101, and the second CT state has a comparable TPA cross section. The results for a model compound of PRL-101, showed the TPA cross sections of its trimer to be

only 1.64 times the monomer value. The ratios we have obtained are much smaller than what have been found in the experiment for PRL-101, PRL-501 and PRL-701, for which a ratio of 1:3.1:6.8 was reported at the fundamental wavelength of 796 nm with a 173 fs pulse length [38].

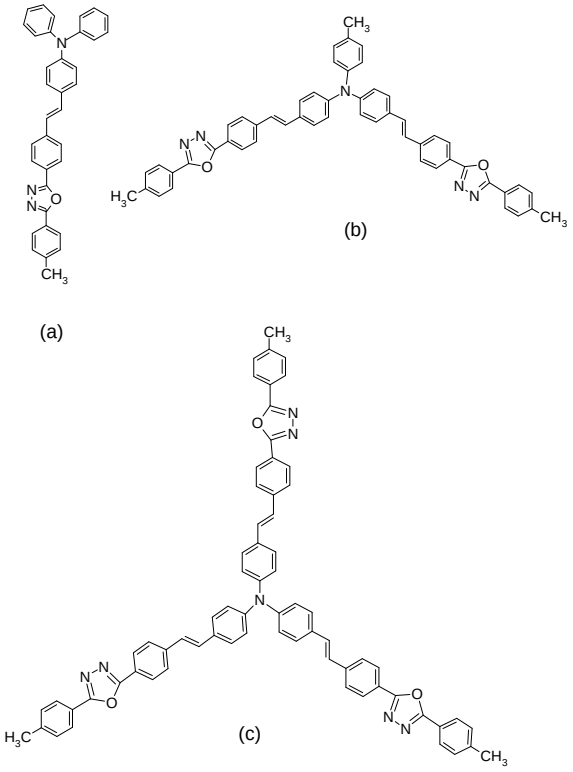

Figure 5.6: Structures of molecule (a) monomer PRL-101; (b) dimer PRL-501 and (c) trimer PRL-701.

It thus seems that solely the electronic contributions can not give rise to the strong enhancement observed in the experiment for the TPA cross sections of the multi-branched molecules studied in this thesis and in [38]. Therefore we have chosen relatively small sized compounds of similar type to investigate the vibronic contributions to the TPA cross sections [38]. In general, the vibronic contributions for the monomer

can be very small, as illustrated in Fig. 5.7 for monomer D′. However, for the dimer, they can be even larger than their electronic counterpart. We have found that the modes involving large displacements of the CC and CN bonds provide the largest contributions. This is certainly understandable since such vibrational movements change the bond-length alternation (BLA) of the molecule. It is known that TPA cross sections, as well as other NLO properties, in general are sensitive to the change of the bond length alternation (BLA) (paper V). By including the vibronic contributions, the ratio between TPA cross sections of the dimer and monomer can thus be enhanced. The absolute value of the vibronic TPA cross section is dependent on the coupling of excited states through the vibrational modes, e.g. the vibronic intensity is borrowed from other electronic states. If other excited states are energetically close and possess large TPA cross sections, large vibronic contributions to the TPA cross section can thus be anticipated. For PRL-501, the energy difference is only 0.2 eV, much smaller than the value of 0.5 eV for dimer D′. It can be anticipated that the vibronic TPA cross sections will be even larger in PRL-501 and PRL-701 due to the high density of states close to the first excited state.

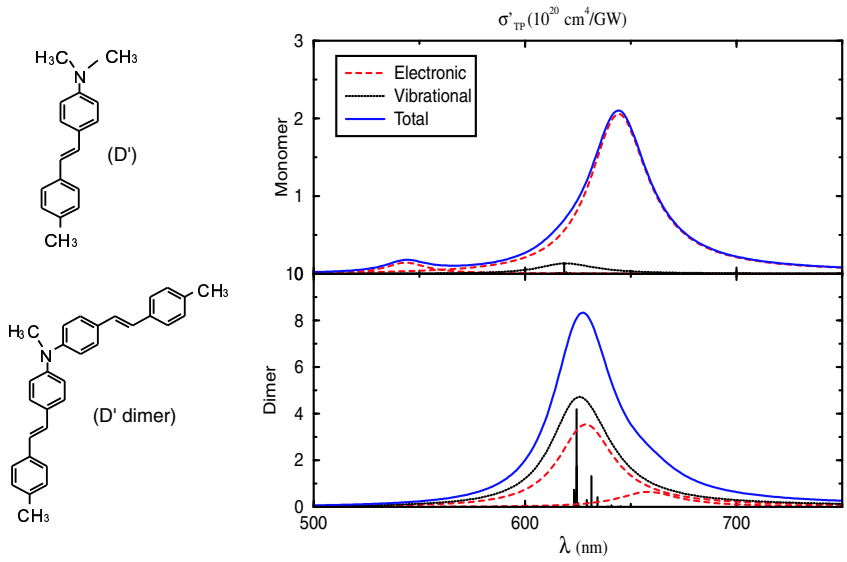

Figure 5.7: Vibronically resolved TPA spectra of the monomer and dimer of compound **D′**. Lifetime broadening was 0.1 eV.

The vibronic contributions to TPA of multi-branched molecules were calculated

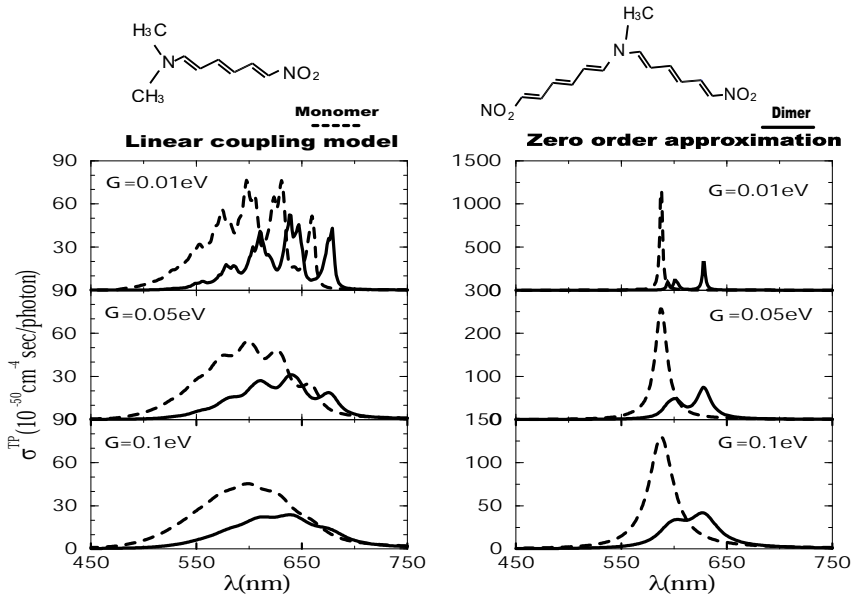

Figure 5.8: Calculated two-photon absorption spectra in the linear coupling model and the zero order harmonic approximation for different lifetime broadenings $\Gamma_F = 0.01$ eV, $\Gamma_F = 0.05$ eV, and $\Gamma_F = 0.1$ eV.

at the zero-order harmonic approximation with no assumption of a change in potential surfaces following the electronic two-photon transition, and they therefore lack any Franck-Condon distribution of the vibronic profile. In order to get a realistic TPA vibronic profile, a higher order approximation has to be introduced. As a first attempt, we have implemented the so-called linear coupling model to simulate the TPA vibronic profiles, which enables to account for both the Herzberg-Teller and the Franck-Condon contributions (paper VII).

The simulations have been carried out for the first excited state of a monomer and a dimer assuming different lifetime broadening shown in Fig. 5.8. It should be stressed that by using response theory, one can in principle obtain vibronic profiles for as many excited states as one wants from a single calculation. It is because the key parameter that needs to be computed in the linear coupling model is the gradient of the excitation energies, which can be obtained from single linear response calculations. The linear coupling model provides a different picture comparing with that from the zero-order harmonic model, with more vibronic structures appearing in the Franck-Condon region. Both the monomer and the dimer possess large numbers of vibrational modes resulting in a high density of vibrational states. The final vibronic

profiles of the TPA spectra of both molecules therefore show only a small number of resolved structures. The vibronic profiles will evidently become broader when the lifetime of the excited state is decreased.

5.6 Dynamics

The modeling of the two-photon absorption cross section concerns usually only the coherent one-step two-photon process. However, when the two-photon absorption cross section is measured, the result often represents the combined effects of coherent two-photon absorption together with other effects. It is especially remarkable that the measured values of two-photon absorption differ by orders of magnitude when measured by different pulse lengths [38]. One of the issues that influences the outcome of the measurement is the effect of saturation related to the lifetimes of the excited states and duration and intensity of the measuring pulses. Another issue is the coherence and in particular the role of incoherent many-step contributions to the nonlinear absorption. Especially in the condensed phase the decoherence processes are in general very fast and one needs to account for a dephasing broadening of resonances, which then probably becomes the main medium effect for two-photon absorption. In order to describe such effects on the measured two-photon absorption cross section we have to study the dynamics of the nonlinear absorption in molecules.

5.6.1 Characteristic times

The dynamics of two-photon absorption of the molecules in solution can be performed with the help of the density matrix formalism (briefly outlined in Sec. 2.2.3). An analytical solution for the time development of the density matrix is impossible to obtain in the general case. A key to the successful solution of the dynamic problem is an analysis of the characteristic times for a particular experimental situation.

For organic molecules in solutions there are known characteristic timescales on which different relaxation processes in the excited states occur. We have in mind here large organic molecules in solvent environments. The states of interest for us are mostly the lowest singlet states S_1, S_2, ... S_n. A general situation is that after excitation to any of these states the molecule rapidly relaxes to the first excited state S_1 (Fig 5.9). This is due to the strong vibrational interactions giving rise to radiationless transitions on the timescale of picoseconds. In contrast, the lifetime of the S_1 state is often much larger - of the order of nanoseconds when determined by the radiation transition to S_0.

If the molecule contains a heavier element the intersystem crossing from the lowest excited singlet S_1 to the lowest excited triplet state T_1 might effectively occur due to spin-orbit interaction. The transition $T_1 \rightarrow S_0$ is spin forbidden with weak radiation transitions called phosphorescence and takes place on a long timescale. This might

also be associated with an efficient excited state absorption in the manifold of triplet states.

The offdiagonal terms Γ_{ij} in the equations for the time development of the density matrices (see Sec. 2.2.3) are typically around 0.1-0.01 eV, which corresponds to the femtosecond time scale. It is interesting to note that the correct order of magnitude for this dephasing rate of molecules in solutions can be obtained from the formula which is strictly valid only for the gas phase - $\Gamma_{ij} \approx \gamma_{ij} \approx \overline{v}\sigma_{ij}N_{tot}$, where $\overline{v}$ is the thermal velocity, σ_{ij} the cross section for the dephasing collisions and N_{tot} the total concentration of molecules.

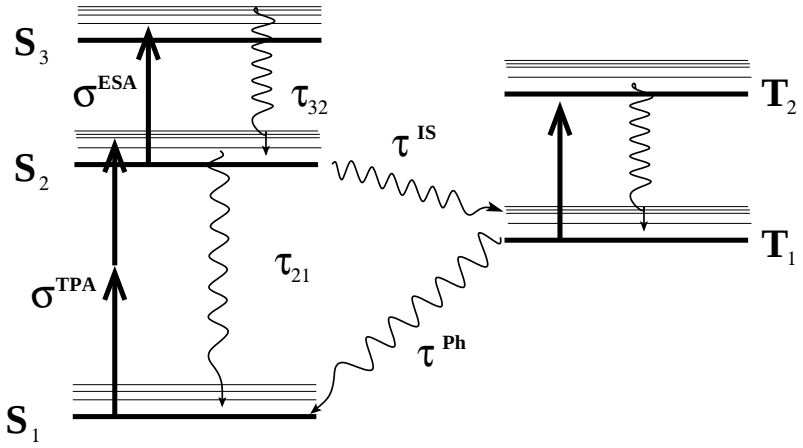

Figure 5.9: Dynamical processes in the population of the excited states of an organic molecule.

5.6.2 Modeling of nonlinear absorption

The pulse lengths used in the measurements can be found in a broad range of times. In the papers X and XI we are modeling an experimental measurement carried out with the pulse lengths 173 fs and 8 ns for the PRL-101 molecule [38]. For both these pulse lengths we can write

$$\Gamma_{jj}^{-1} > \tau_p > \Gamma_{ij}^{-1}. \tag{5.29}$$

This considerably simplifies the solution of the kinetic equations for populations and off-diagonal elements of the density matrix

$$\left(\frac{\partial}{\partial t} + \Gamma_{ii}\right)\rho_{ii} = \sum_{\alpha}\tilde{\Gamma}_{\alpha\alpha}\rho_{\alpha\alpha} + i\left[\rho, V\right]_{ii}, \qquad \left(\frac{\partial}{\partial t} + \Gamma_{\alpha\alpha}\right)\rho_{\alpha\alpha} = i\left[\rho, V\right]_{\alpha\alpha},$$

$$\left(\frac{\partial}{\partial t}+\Gamma_{ij}\right)\rho_{ij} \quad = \quad i\left[\rho,V\right]_{ij}, \qquad Tr\rho = N, \qquad\qquad V=-\mathbf{E}\boldsymbol{\mu}. \tag{5.30}$$

Here the nonradiative conversion rate $\tilde{\Gamma}_{\alpha\alpha}$ of the decay transition $\alpha \rightarrow i$ is large in organic molecules and almost completely coincides with the total decay $\Gamma_{\alpha\alpha}$. From the solutions of these equations we can find the total polarization. The equation for the intensity or irradiance then becomes

$$\left(\frac{\partial}{\partial z}+\frac{1}{c}\frac{\partial}{\partial t}\right)I \quad = \quad -N\left(\sigma^{(1)}I+\sigma^{(2)}I^2+\sigma^{(3)}I^3\right), \qquad \sigma^{(2)}=\sigma_1^{(1)}+\sigma_2^{(2)}. \tag{5.31}$$

Here $\sigma^{(1)}$, $\sigma^{(2)}$ and $\sigma^{(3)}$ are one-, two- and three-photon absorption cross sections respectively. There are two contributions to the effective two-photon absorption absorption (see Fig. 5.10). The first one is the coherent one-step TPA $\sigma_1^{(2)}$ which we already have discussed (see Eq. (5.4)). The second part, $\sigma_2^{(2)}$, is the incoherent two-step TPA. The expressions for $\sigma_2^{(2)}$ and $\sigma^{(3)}$ can be found in paper X. Contrary to $\sigma_1^{(2)}$, the two-step contribution $\sigma_2^{(2)}$ is directly related to the off-resonant population, $0 \rightarrow j$, of the states $j=(i,\alpha)$.

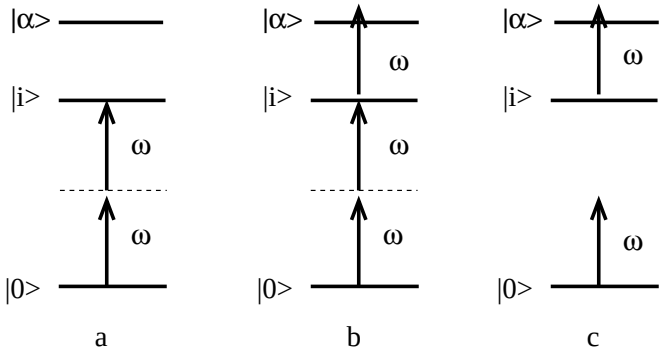

Figure 5.10: Different nonlinear absorption mechanisms. (a) Coherent one-step two-photon absorption. (b) Three-photon absorption. (c) Incoherent two-step two-photon absorption.

5.6.3 Saturation effects

The experiments with long pulses [39, 40, 38] which we analyze in paper X, were not performed for weak intensities, something that calls for an account of saturation effects. These effects will decrease the TPA cross section. The strict solution of the density matrix equations for arbitrary intensities poses a quite complicated problem due to the existence of a set of different saturation intensities. The simplest way to

take into account the saturation is through the particle conservation law related to the equations for populations:

$$(\frac{\partial}{\partial t} + \Gamma_{ii})\rho_{ii} = \sum_{\alpha} \tilde{\Gamma}_{\alpha\alpha}\rho_{\alpha\alpha} + \frac{\Gamma_{ii}}{2}\kappa_{i0}(\rho_{00} - \rho_{ii}) + \Gamma_{ii}\sum_{\alpha}\kappa_{\alpha i}(\rho_{\alpha\alpha} - \rho_{ii}),$$
$$(\frac{\partial}{\partial t} + \Gamma_{\alpha\alpha})\rho_{\alpha\alpha} = \Gamma_{ii}\kappa_{\alpha i}(\rho_{ii} - \rho_{\alpha\alpha}) + \Gamma_{ii}\kappa_{\alpha 0}(\rho_{00} - \rho_{\alpha\alpha}). \tag{5.32}$$

The rates of radiative transition ($0 \to i$, $0 \to \alpha$, $i \to \alpha$) are proportional to the corresponding saturation parameters

$$\kappa_{ij} = \frac{I}{I_{ij}}, \tag{5.33}$$

which is the ratios of the intensity to the corresponding saturation intensities I_{ij}. Detailed expressions for the saturation intensities can be found in paper X.

A recent nonlinear absorption measurement on the PRL-101 molecule [38] resulted in an effective two-photon absorption cross section 171 times higher when measured with the 8ns pulse than when measured with the 173 fs pulse. With the transition moments calculated by *ab initio* methods we have simulated in paper X the dependence of the ratio of the measured effective TPA cross sections for long and short pulses with respect to the intensity of the pulse (Fig. 5.11).

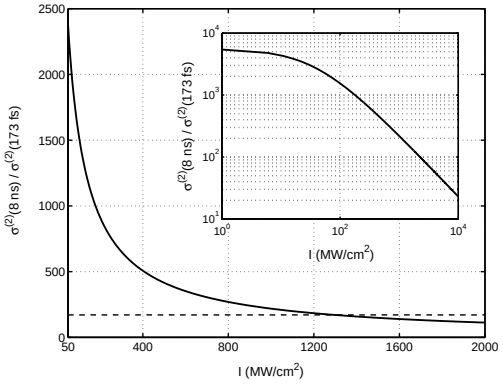

Figure 5.11: The intensity dependence of the ratio of the TPA cross sections $\sigma^{(2)}$ for long (8 ns) and short (173 fs) pulses. The experimental value, $\sigma^{(2)}$(8 ns)/$\sigma^{(2)}$(173 fs)=171, is shown by dashed line.

The experimental measurements are found to be performed under strong saturation conditions. The effective two-photon absorption is shown to be completely dominated by incoherent two-step two-photon absorption $\sigma_2^{(2)}$ for measurements with the long pulse. The main reason for this is the large dephasing rate Γ_{ij} caused by the solvent compared to the lifetime of the excited state.

Chapter 6

Solvent effects

While calculations of nonlinear optical properties are most easily performed for isolated molecules, many experimental measurements take place in the condensed phase. A solvent environment modifies the properties of solvated molecules and has at the same time a significant influence on the dynamics of the processes.

From the point of view of the nonlinear optical response of molecules the most important influences due to the solvent environment are following:

- The **molecular wave function and structure change** in the perturbing environment. If the solute molecule has a dipole moment it polarizes the solvent molecules around it which affects in return the solute molecular wave function. Also short range interactions, like exchange interaction or hydrogen bonding influence the molecular wave function. The geometrical structure of the molecule may also be changed significantly.

- The **response properties of the molecule are different** due to the presence of the solvent environment.

- The **perturbing local field acting on the molecule is changed.** The solvent molecules screen the macroscopic field and the field acting on a molecule is no longer the pure external Maxwell field, but a so-called local field.

- The **dynamics of the excitation processes** is influenced by the solvent environment. The interactions and collisions with the solvent molecules have crucial effects on dephasing factors and lifetimes of the excited states of the solvated molecules.

6.1 Modeling strategies

Compared to the calculation of properties of an isolated molecule, the calculation of properties of molecules in a condensed environment presents a giant task - the number of molecules involved is huge. Typical numbers are of the order of Avogadros number - 10^{23} particles. We really have to assume some substantial simplifications.

There are two fundamentally different ways of representing the solvent environment - the discrete and the continuum approaches (see Fig. 6.1).

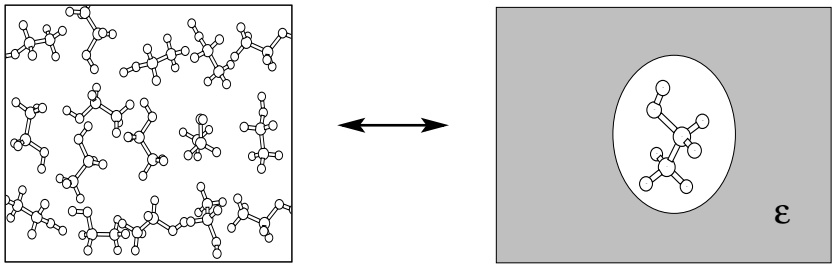

Figure 6.1: Continuum versus discrete models for solution. In discrete models we have to either restrict to small clusters of molecules or treat a large part of the molecules in a more classical way. In the dielectric continuum model the medium effect on the solvent molecules is approximated by a homogeneous dielectric continuum.

Discrete models

- **Supermolecular approach.** Here one describes a molecule with some of the neighboring solvent molecules and treats all of these in a quantum mechanical way. The short term specific interactions like hydrogen bondings can be treated in this way.
- **Molecular Mechanics.** The response to the perturbing fields of individual molecules are described in terms of polarizabilities etc. which can be calculated or fitted empirically. In an ensemble of molecules the classical electrostatic interactions are evaluated between the charge distributions of the molecules (point charges, dipoles, etc.). Even other types of interactions like the van der Waals interaction can be included. The charge distributions of an individual molecule changes due to the interactions with other molecules. Thus the overall charge distributions of an ensemble of molecules has to be calculated self-consistently.
- **Hybrid quantum mechanics/molecular mechanics method (QM/MM).** In this method one or a few molecules are treated quantum mechanically, while the

surrounding molecules are described in the classical molecular mechanical way.

- **Molecular Dynamics.** The theoretically or empirically fitted intermolecular potentials are used in the Newtons classical equations of motion for modeling the trajectories of the molecules. A statistical averaging of the property over generated configurations is used.
- **Monte Carlo method.** An algorithm based on the Boltzmann factor determining the probability of a certain configuration can be used for generating a set of configurations suitable for evaluating the property in a statistical manner.

Dielectric continuum models

These models approximate the solvent environment by a homogeneous dielectric continuum characterized by its dielectric constant ϵ. Both static and frequency dependent dielectric constants can be used in the models.

- **Onsager reaction field model.** The molecule in solution is modeled as a classical point polarizable dipole in a spherical, or more generally, ellipsoidal cavity surrounded by a dielectric continuum.
- **Self-consistent reaction field model** (SCRF). The solute molecule is treated quantum mechanically as embedded in a spherical cavity inside a dielectric continuum. The molecular charge distribution is inducing polarization in a continuum, which acts back on the molecule in terms of the reaction field. The molecular charge distribution is influenced by this reaction field and has to be determined self-consistently with the reaction field it is inducing.
- **Polarizable continuum model** (PCM). The solute molecule is treated quantum mechanically in a cavity around it that assumes a molecular shape.

There exist also semi-continuum models which mix the continuum approach with the discrete description of nearest neighboring molecules including the first solvation shell.

6.2 Dielectric continuum models

In this work the continuum model is used as a starting point because of its ability to account for long range polarization interactions which is crucial for the nonlinear optical properties and because of its conceptual and computational simplicity. We adopt the continuum approach, which describes the solute molecule as a molecule inside a cavity embedded in a homogeneous dielectric continuum. This dielectric continuum is characterized by its static and/or dynamic dielectric constant ϵ. No overlap of electronic clouds of the molecule with surrounding molecules is considered. Thus the

short range repulsive and specific interactions (like hydrogen bonding) are not included explicitly in this model and only the long-range polarization interactions are included. The basic expressions in the continuum model origin from the solution of Maxwell equations of a cavity in a dielectric either with or without a charge distribution inside it.

The history of the continuum models goes back to the beginning of previous century, to the basic ideas of Born, Kirkwood and Onsager [41, 42, 43]. They started with a picture of a molecule in a spherical cavity surrounded by a homogeneous dielectric continuum. Solutions of Maxwell equations for the cavity problems [16, 44] are used to describe the connection between the fields acting on the molecule, the external fields and the molecular multipole moments. Despite being a relatively crude approximation the continuum model has been successfully applied in many areas of physics and chemistry. A very good summary of the classical theory of polarization can be found in the book by Böttcher [16].

In the Onsager (dipolar) model only dipole interactions are considered. The dipole moment of the molecule polarizes the continuum around it and this gives rise to a field acting back on the molecule - a reaction field. Generalizations of the dipolar reaction field model for the higher multipolar moments together with a quantum mechanical treatment of the molecule gave rise to a number of self-consistent reaction field models (SCRF) models [45, 46, 47]. This name comes from the fact that the charge distribution of the molecule has to be determined self-consistently with the reaction field it has induced. Cavities of molecular shapes have been included in the approach known as the polarizable continuum model (PCM) [48, 49, 50, 51]. For a discussion on current approaches based on continuum models we refer to the review of Tomasi and Persico [52].

6.2.1 Onsager reaction field model

In the original Onsager reaction field model only dipolar reaction terms were included. The molecule is represented as a point polarizable dipole in a spherical cavity immersed in a homogeneous dielectric continuum characterized by its dielectric constant ϵ.

The dipole moment of the molecule polarizes the surrounding which gives rise to the reaction field acting back on the molecule. Thus even in the absence of any external field, there is still (for a polar molecule) a reaction field acting on the molecule [see Fig. 6.2(a)]. The connection between the dipole moment and the reaction field is linear. For a spherical cavity with the radius a we have

$$F_i^{\mathrm{R}} \quad = \quad f^{\mathrm{R}} p_i, \qquad f^{\mathrm{R}} = \frac{1}{a^3} \frac{2(\epsilon_1 - 1)}{2\epsilon_1 + 1}, \tag{6.1}$$

where the f^{R} is called the reaction field factor.

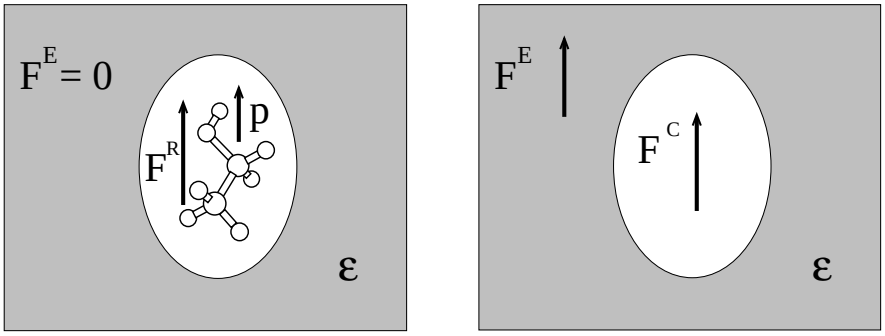

(a) $F_i^{\mathrm{R}} = f_{ij}^{\mathrm{R}} p_j$ (b) $F_i^{\mathrm{C}} = f_{ij}^{\mathrm{C}} F_j^{\mathrm{E}}$

Figure 6.2: A dielectric continuum (a) surrounding a cavity containing a molecule a and (b) surrounding an empty cavity.

On the other hand, having an empty cavity an applied external field $\mathbf{F}^{\mathrm{E}}$ will give rise to a cavity field inside this cavity [see Fig. 6.2(b)]. There is also a linear connection between the cavity field $\mathbf{F}^{\mathrm{C}}$ and the external field $\mathbf{F}^{\mathrm{E}}$. For a spherical cavity

$$F_i^{\mathrm{R}} = f^{\mathrm{C}} F_i^{\mathrm{E}}, \qquad f^C = \frac{3\epsilon_1}{2\epsilon_1 + 1}, \tag{6.2}$$

where f^{C} is the cavtity field factor.

For an ellipsoidal cavity, the reaction field and cavity factors become tensors. In the ellipsoidal cavity with semiaxes a_x, a_y and a_z, the solution can be obtained by solving the Laplace equation in ellipsoidal coordinates [44, 16]

$$f_{ij}^{\mathrm{R}} = \frac{3}{a_x a_y a_z} \frac{\kappa_i(1-\kappa_i)(\epsilon-1)}{\epsilon + (1-\epsilon)\kappa_i} \delta_{ij}, \tag{6.3}$$

$$f_{ij}^{C} = \frac{\epsilon}{\epsilon - \kappa_i(\epsilon-1)} \delta_{ij}, \tag{6.4}$$

where κ_r is defined as

$$\kappa_i = \frac{a_x a_y a_z}{2} \int_0^\infty ds \left[(s+a_x^2)(s+a_y^2)(s+a_z^2)\right]^{-1/2} (s+a_i^2)^{-1}, \tag{6.5}$$

fulfilling the condition $\kappa_x + \kappa_y + \kappa_z = 1$. For a spherical cavity we have κ_i=1/3.

All factors we presented here are diagonal, but in a more general case the factors might be nondiagonal. Numerical methods have been developed to account for more general shapes of the cavity [53].

From the superposition principle it follows that for a given external field $\mathbf{F}^{\mathrm{E}}$ and certain dipole moment $\mathbf{p}$ the total local field acting on the molecule is a sum of the cavity and the reaction fields belonging to that particular dipole moment

$$F_i^L = F_i^R + F_i^C. \tag{6.6}$$

All these expressions for the reaction field and the local field are valid for arbitrary molecular dipole moments. If the molecule is in a solvent environment without an external perturbation, a certain *self-consistent* value of the dipole moment is established. This value, which we denote $\boldsymbol{\mu}^{\mathrm{sol}}$, would be different from the gas phase value $\boldsymbol{\mu}^0$ for polar molecules. This solute molecular dipole moment $\boldsymbol{\mu}^{\mathrm{sol}}$ creates a certain initial reaction field which we denote by $\mathbf{F}^{\mathrm{R}_0}$.

If we approximate the molecule as a point polarizable dipole and neglect all the nonlinear terms in Eq. (2.15) we get an additional relation between $\boldsymbol{\mu}^{\mathrm{sol}}$ and $\mathbf{F}^{\mathrm{R}_0}$. Together with Eq. (6.1) this gives us a system of two equations that has to be solved simultaneously

$$\mu_i^{\mathrm{sol}} = \mu_i^0 + \alpha_{ij}^0 F_j^{\mathrm{R}_0}, \tag{6.7}$$

$$F^{\mathrm{R}_0} = f_{ij}^{\mathrm{R}} \mu_j^{\mathrm{sol}}. \tag{6.8}$$

Extracting $\boldsymbol{\mu}^{\mathrm{sol}}$ from them gives

$$\mu_i^{\mathrm{sol}} = (\mathbf{1} - \boldsymbol{\alpha}\boldsymbol{f}^{\mathrm{R}})_{ij}^{-1} \mu_j^0. \tag{6.9}$$

The latter equation offers a possibility to define a reaction field factor for the polarizable dipole as

$$\mathbf{f}^{\mathrm{PD}} = (\mathbf{1} - \boldsymbol{\alpha}\boldsymbol{f}^{\mathrm{R}})^{-1}, \tag{6.10}$$

with the property similar to the reaction field factor $\mathbf{f}^{\mathrm{R}}$ that reads

$$F_i^{\mathrm{R}_0} = f_{ij}^{\mathrm{PD}} \mu_j^0, \tag{6.11}$$

where $\boldsymbol{\mu}^0$ is the gas phase dipole moment and $\mathbf{F}^{\mathrm{R}_0}$ is the initial reaction field. In the case when the nonlinear behavior of the molecule is not neglected the solute dipole moment can be determined self-consistently from Eqs. (6.27)-(6.28).

For the static case it is useful to define also a local induced field which is the difference between the local field with and without an external field

$$F_i^{\mathrm{L_I}} = F_i^{\mathrm{R_I}} + F_i^{\mathrm{C}}, \qquad F_i^{\mathrm{R_I}} = f_{ij}^{\mathrm{R}} p_j^{\mathrm{ind}}, \tag{6.12}$$

where $\mathbf{p}^{\mathrm{ind}}$ is the part of the dipole moment induced by application of the external field. The difference to the local field is only due to the initial reaction field $\mathbf{F}^{\mathrm{R}_0}$.

For a frequency dependent field there is no such problem since all the fields involved are induced (there are no frequency dependent fields when the external field is off)

$$F_i^{\mathrm{L}\omega} = F_i^{\mathrm{R}\omega} + F_i^{\mathrm{C}\omega}, \qquad F_i^{\mathrm{R}\omega} = f_{ij}^{\mathrm{R}\omega} p_j^{\omega}. \tag{6.13}$$

Energy of solvated molecules

The energy of a molecule in a cavity surrounded by a dielectric consists of three parts: the energy of the molecule itself E^0 (the energy of the isolated molecule in the same internal state); the energy necessary to create the cavity E^{C} and the energy necessary to bring the isolated molecule to the cavity denoted by W^{sol}.

Since E^{C} is constant it would not influence other properties of the molecule. Due to the fact that we are concerned with nonlinear optical properties in this thesis, we will include in the solute molecule energy E^{sol} just the two remaining contributions, skipping E^{C}.

Both E^0 and W^{sol} are in this definition dependent on the actual state of the molecule - its dipole moment $\mathbf{p}$

$$E^{sol}(\mathbf{p}) = E^0(\mathbf{p}) + W^{sol}(\mathbf{p}). \tag{6.14}$$

In general not only dipole interactions contribute to the energy, but also higher multipolar expansions. However, usually for uncharged molecules the dipolar contribution is dominant [54].

For an arbitrary molecular dipole moment $\mathbf{p}$, the energy W^{sol} needed to bring the isolated molecule in a particular state inside the cavity can be expressed as $-\frac{1}{2}p_i F_i^{\mathrm{R}}$ [16], or using the relation between the reaction field and the dipole moment (6.1)

$$W^{\mathrm{sol}}(p) = -\frac{1}{2}p_i f_{ij}^{\mathrm{R}} p_j. \tag{6.15}$$

The factor one-half appears since the reaction field is not constant but instead proportional to the dipole moment in the process of assembling the charge distribution inside the cavity.

When the external field is turned on, the cavity field is induced and the energy of the molecule is changed in two ways: first, the dipole moment p changes (self-consistently) and thus also $E^0(p)$ and $W^{sol}(p)$ change correspondingly; second, the potential energy of the newly established dipole moment $\mathbf{p}$ in the cavity field $\mathbf{F}^{\mathrm{C}}$ must be added

$$E^{sol}(\mathbf{p}) = E^0(\mathbf{p}) + W^{sol}(\mathbf{p}) - p_i F_i^{\mathrm{C}}. \tag{6.16}$$

This is an important result which we will benefit from in the discussion of the quantum mechanical models in this thesis. The dipole moment $\mathbf{p}$ is established self-consistently for each applied cavity field $\mathbf{F}^{\mathrm{C}}$. It will be different from the gas phase value $\boldsymbol{\mu}^0$ and also from the initial solute value $\boldsymbol{\mu}^{\mathrm{sol}}$.

For the case of no external fields the dipole moment $\mathbf{p}$ of the molecule is equal to the solute dipole moment $\boldsymbol{\mu}^{\mathrm{sol}}$ given by Eq. (6.9) or by Eqs. (6.27) and (6.28). In this case it is possible, using the approximation (6.9), to express the solvation energy E^{sol} in terms of gas phase properties. The change of $E^0(\boldsymbol{\mu}^{\mathrm{sol}})$ in the linear approximation is

$$E^0(\boldsymbol{\mu}^{\mathrm{sol}}) - E^0(\boldsymbol{\mu}^0) \quad = \quad \frac{1}{2}\alpha_{ij}^0 F_i^{\mathrm{R}_0} F_j^{\mathrm{R}_0},$$

$$= \frac{1}{2}(\mu_i^{\mathrm{sol}} - \mu_i^0)F_i^{\mathrm{R_0}}. \tag{6.17}$$

Using the definition of the reaction field factor for a polarizable dipole (6.10) we can rewrite this result in terms of only gas phase properties

$$E^{sol} = E^0(\boldsymbol{\mu}^0) - \frac{1}{2}\mu_i^0 F_j^{\mathrm{R_0}}, \tag{6.18}$$

$$E^{sol} = E^0(\boldsymbol{\mu}^0) - \frac{1}{2}\mu_i^0 f_{ij}^{\mathrm{PD}}\mu_j^0. \tag{6.19}$$

6.2.2 Self-consistent reaction field model

The charge distribution inside the cavity induces a reaction field and potential V_{pol} in the dielectric. The induced field interacts with the charge distribution ρ inside the cavity. The resulting polarization energy (or solvent energy) is given by

$$E_{\mathrm{pol}} = \frac{1}{2}\int d\mathbf{r}\rho(\mathbf{r})V_{\mathrm{pol}}. \tag{6.20}$$

By solving the Maxwell equations with the boundary condition for a cavity with radius a surrounded by the dielectric continuum with dielectric constant ϵ we can obtain an expression for the polarization energy as a summation over a multipole expansion

$$E_{pol} = \sum_{l=0}^{\infty} U_l, \tag{6.21}$$

where

$$U_l = -\frac{1}{2}g_l \sum_{m=-l}^{l} (-1)^m M_l^{-m} M_l^m, \tag{6.22}$$

$$g_l = \frac{1}{a^{2l+1}}\frac{(l+1)(\epsilon-1)}{l+\epsilon(l+1)}, \tag{6.23}$$

$$M_l^m = \int d\mathbf{r}\rho(\mathbf{r})S_l^m(\mathbf{r}), \tag{6.24}$$

$$S_l^m = \sqrt{\frac{4\pi}{2l+1}}r^l Y_{l,m}(\theta,\phi). \tag{6.25}$$

Here $Y_{l,m}$ are spherical harmonic functions. Usually, the expansion in Eq. (6.21) converges quite quickly and only terms up to $l = 6$ have to be taken into account in this thesis. As discussed above the reaction field induced by the charge distribution of the molecule interacts back with the molecule. Thus it has to be calculated *self-consistently* with this reaction field. This can be achieved by an iterative procedure starting with the charge distribution of the isolated molecule and correcting it for the reaction field effect in each iteration. After a few iterations the self-consistency is normally reached.

6.3 Solvent effects on nonlinear optical properties

6.3.1 Definitions of the properties

The molecular nonlinear optical properties are defined by the Taylor expansion of the total dipole moment in orders of the strength of a perturbing field $\mathbf{F}$

$$\mu_i^{tot} = \mu_i + \alpha_{ij}F_j + \frac{1}{2}\beta_{ijk}F_jF_k + \frac{1}{6}\gamma_{ijkl}F_jF_kF_l + \cdots. \tag{6.26}$$

In the absence of the external field $\mathbf{F}^{\mathrm{E}}$ the solute dipole moment $\boldsymbol{\mu}^{\mathrm{sol}}$ of the molecule gives rise, in the dipolar approximation, to the *initial reaction field* $\mathbf{F}^{\mathrm{R}_0}$

$$F_i^{\mathrm{R}_0} = f_{ij}^{\mathrm{R}}\mu_j^{\mathrm{sol}}, \tag{6.27}$$

$$\mu_j^{\mathrm{sol}} = \mu_j + \alpha_{jk}F_k^{\mathrm{R}_0} + \frac{1}{2}\beta_{jkl}F_k^{\mathrm{R}_0}F_l^{\mathrm{R}_0} + \cdots, \tag{6.28}$$

where $\boldsymbol{\mu}, \boldsymbol{\alpha}, \boldsymbol{\beta}, \ldots$ are the gas phase dipole moment, polarizability and hyperpolarizability of the molecule, and $\mathbf{F}^{\mathrm{R}_0}$ is the reaction field induced by the initial solute dipole moment μ^{sol} (without external field).

In the presence of an external field $\mathbf{F}^{\mathrm{E}}$ the induced dipole moment can be expanded in terms of different fields which can easily lead to confusion in the definition of molecular properties in solution. In the literature, three different fields, namely the *external* Maxwell field $\mathbf{F}^{\mathrm{E}}$, the *cavity* field $\mathbf{F}^{\mathrm{C}}$ and the *local induced* field $\mathbf{F}^{\mathrm{L_I}}$ have been used, which lead to *effective*, *cavity* and *local* field properties respectively [55]

$$F_i = \begin{cases} F_i^{\mathrm{E}} & \rightarrow \textit{ effective properties} \\ F_i^{\mathrm{C}} & \rightarrow \textit{ cavity field properties} \\ F_i^{\mathrm{L_I}} & \rightarrow \textit{ local field properties} \end{cases}. \tag{6.29}$$

The *local field properties* (LFP) are the properties that can be expressed in terms of a perturbation expansion in the *initial reaction field* $\mathbf{F}^{\mathrm{R}_0}$

$$\alpha_{ij}^{\mathrm{L}}(-\omega;\omega) = \alpha_{ij}(-\omega;\omega) + \beta_{ija}(-\omega;\omega,0)F_a^{\mathrm{R}_0} + \frac{1}{2}\gamma_{ijab}(-\omega;\omega,0,0)F_a^{\mathrm{R}_0}F_b^{\mathrm{R}_0} + ..., \tag{6.30}$$

$$\beta_{ijk}^{\mathrm{L}}(-2\omega;\omega,\omega) = \beta_{ijk}(-2\omega;\omega,\omega) + \gamma_{ijka}(-2\omega;\omega,\omega,0)F_a^{\mathrm{R}_0} + ..., \tag{6.31}$$

$$\gamma_{ijkl}^{\mathrm{L}}(-3\omega;\omega,\omega,\omega) = \gamma_{ijkl}(-3\omega;\omega,\omega,\omega) + \delta_{ijkla}(-3\omega;\omega,\omega,\omega,0)F_a^{\mathrm{R}_0} + ... \tag{6.32}$$

where $\mathbf{F}^{\mathrm{R}_0}$ is determined from Eqs. (6.27) and (6.28). It is these properties that experimentalists usually refer to as solute properties.

Cavity field properties (CFP) are on the other hand properties that usually come out of theoretical calculations. Self-consistent reaction field methods, which incorporate

the induced reaction field in the unperturbed part of the Hamiltonian rather than as a perturbation, provide solute properties belonging to this category. Starting from the general expansion of the dipole moment, the following connection to the *local field properties* can be derived [55]

$$\alpha^{\mathrm{C}}_{ij}(-\omega;\omega) = l^{\omega}_{ia}\ \alpha^{\mathrm{L}}_{aj}(-\omega;\omega), \tag{6.33}$$

$$\beta^{\mathrm{C}}_{ijk}(-2\omega;\omega,\omega) = l^{2\omega}_{ic} l^{\omega}_{ja} l^{\omega}_{kb}\ \beta^{\mathrm{L}}_{cab}(-2\omega;\omega,\omega), \tag{6.34}$$

$$\begin{aligned}\gamma^{\mathrm{C}}_{ijkl}(-3\omega;\omega,\omega,\omega) = {} & l^{3\omega}_{id} l^{\omega}_{ja} l^{\omega}_{kb} l^{\omega}_{lc}\ \gamma^{\mathrm{L}}_{dabc}(-3\omega;\omega,\omega,\omega) \\ & +\beta^{\mathrm{L}}_{ija}(-3\omega;\omega,2\omega) f^{\mathrm{R}\omega}_{ab} \beta^{\mathrm{C}}_{bkl}(-2\omega;\omega,\omega) \\ & +\beta^{\mathrm{L}}_{ika}(-3\omega;\omega,2\omega) f^{\mathrm{R}\omega}_{ab} \beta^{\mathrm{C}}_{bjl}(-2\omega;\omega,\omega) \\ & +\beta^{\mathrm{L}}_{ila}(-3\omega;\omega,2\omega) f^{\mathrm{R}\omega}_{ab} \beta^{\mathrm{C}}_{bjk}(-2\omega;\omega,\omega)\end{aligned} \tag{6.35}$$

where $l^{n\omega}_{ij} = \delta_{ij} + f^{\mathrm{R}n\omega}_{ia} \alpha^{\mathrm{C}}_{aj}(-n\omega;n\omega)$.

6.3.2 Quantum mechanical models

In order to calculate the response of a molecule to the external perturbation, the Hamiltonian is divided into an unperturbed part, including the Hamiltonian for the molecule and the solute-solvent interaction, and an external perturbation

$$H = H^{\mathrm{sol}} + H^{\mathrm{pert}}. \tag{6.36}$$

There is a little problem, however, that part of the induced polarization effect can be understood as either contributing to the local field factors or to the change of the solute molecular response properties. To avoid this ambiguity it is better to use effective properties, which describe directly the response of the molecule with respect to the external Maxwell field [13, 56]. We demonstrate this difference in a simple way, including only the dipolar term in the solute-solvent interaction.

Local field as perturbation

The easiest way to incorporate the effect of the reaction field into the Hamiltonian is to use the finite field term

$$H^{\mathrm{sol}} = H^0 - \hat{\mu}_i F^{\mathrm{R}_0}_i, \tag{6.37}$$

where H^0 is the gas phase Hamiltonian, $\hat{\boldsymbol{\mu}}$ is the dipole moment operator, and $\mathbf{F}^{\mathrm{R}_0}$ is the initial reaction field induced by the the self-consistently determined charge distribution of the molecule without any external Maxwell field.

This approach takes care of the initial static reaction field that is always present, but no effects from the induced reaction field are accounted for. Thus, after applying

static or dynamic external fields, the perturbation to be added to this Hamiltonian would be the local induced field

$$H = H^0 - \hat{\mu}_i F_i^{\mathrm{R}_0} - \hat{\mu}_i F_i^{\mathrm{L}_\mathrm{I}}, \tag{6.38}$$

where for dynamic fields $F^{\mathrm{L}\omega}$ would appear instead of $F^{\mathrm{L}_\mathrm{I}}$. The perturbation in this model is the induced local field.

Cavity field as perturbation

Another quantum mechanical approach taking into account the solute-solvent interactions in the continuum models starts from the classical expressions for the total energy of the molecule in its own reaction field (6.16). This approach includes also the induced part of the self-consistent reaction field directly into the Hamiltonian. This means that we have to put a nonlinear term into the Hamiltonian the average of which would give W^{sol} from Eq. (6.15). This type of reaction field methods is commonly assumed in *ab initio* self-consistent reaction field models [45]. Written for the dipolar level, it leads to a Hamiltonian of the form

$$H^{\mathrm{sol}} = H^0 - \frac{1}{2}\hat{\mu}_i f^{\mathrm{R}} \langle \Psi | \hat{\mu}_i | \Psi \rangle, \tag{6.39}$$

where Ψ is the actual wave function of the molecule.

When the external field is absent the Hamiltonians given in Eqs. (6.38) and (6.39) are fully equivalent. Thus the molecular wave function and all the properties related directly to this wave function without introducing any perturbation to the Hamiltonian become the same in both approaches. But when an external field is applied we have to distinguish between the two cases. The problem is that the Hamiltonian (6.39) already includes all of the induced reaction field $\mathbf{F}^{\mathrm{R}_\mathrm{I}}$ and thus the perturbation introduced in this case originates exclusively from the cavity field [cf. Eq. (6.16)]

$$H = H^0 - \frac{1}{2}\hat{\mu}_i f^{\mathrm{R}} \langle \Psi | \hat{\mu}_i | \Psi \rangle - \hat{\mu}_i F_i^{\mathrm{C}}. \tag{6.40}$$

The differences in the interpretation of the properties calculated by these two different Hamiltonians are discussed in paper III. The self-consistent reaction field response method [46] is of this type. It includes higher multipole moments for the description of the solute-solvent interaction and can be generalized for the nonequilibrium situation [47], where the solvent environment is characterized by static and optical dielectric constants.

6.3.3 Semiclassical model

Expressing *cavity field properties* in terms of *gas phase properties* from equations (6.30)-(6.32) and (6.33)-(6.35) would lead to rather complicated formulas. However, using

the classical Onsager expression for the energy of the solvated molecule (6.19) one can under certain approximations derive a simplified set of expressions [54, 57]

$$\begin{aligned}
\mu_i^{\rm sol} &= \mu_i + \mu_m f^R_{mn}\alpha_{ni}, && (6.41)\\
\alpha^C_{ij} &= \alpha_{ij} + \alpha_{im}f^R_{mn}\alpha_{nj} + \mu_m f^R_{mn}\beta_{nij}, && (6.42)\\
\beta^C_{ijk} &= \beta_{ijk} + \alpha_{im}f^R_{mn}\beta_{njk} + \alpha_{jm}f^R_{mn}\beta_{nik} + \alpha_{km}f^R_{mn}\beta_{nij} + \mu_m f^R_{mn}\gamma_{nijk}, && (6.43)\\
\gamma^C_{ijkl} &= \gamma_{ijkl} + \alpha_{im}f^R_{mn}\gamma_{njkl} + \alpha_{jm}f^R_{mn}\gamma_{nikl} + \alpha_{km}f^R_{mn}\gamma_{nijl} + \alpha_{lm}f^R_{mn}\gamma_{nijk} \\
&\quad +\beta_{ijm}f^R_{mn}\beta_{nkl} + \beta_{ikm}f^R_{mn}\beta_{njl} + \beta_{ilm}f^R_{mn}\beta_{njk} + \mu_m f^R_{mn}\delta^e_{nijkl}. && (6.44)
\end{aligned}$$

The reliability of a semi-classical solvation model for optical properties of molecules in solutions have been examined for molecules with small, medium and large size [54, 57, 55].

The semiclassical model can be used also for evaluation of the vibrational contributions to solute NLO properties. For example, the vibrational contributions to the static solute polarizability are in general given by

$$\alpha^{v,{\rm sol}}_{ij} = \frac{\partial\mu^{\rm sol}_i}{\partial Q^{\rm sol}_a}\frac{\partial\mu^{\rm sol}_j}{\partial Q^{\rm sol}_a}/(\omega^{\rm sol}_a)^2, \qquad (6.45)$$

where we sum over all the normal modes of the molecule. Within the cavity approximation it has been shown in many cases that the molecular structure does not change significantly upon solvation, see for instance Refs. [58, 59], and it is therefore reasonable to make the approximation that $\omega^{\rm sol}_a = \omega_a$ and $Q^{\rm sol}_a = Q_a$ [54]. By inserting Eq. 6.41 into Eq. 6.45 and introducing this approximation we obtain

$$\begin{aligned}
\alpha^{v,{\rm sol}}_{ij} &= \alpha^v_{ij} + \alpha^v_{ik}f^R_{kl}\alpha^e_{lj} + \alpha^e_{ik}f^R_{kl}\alpha^v_{lj} + \alpha^e_{ik}f^R_{kl}\alpha^v_{lm}f^R_{mn}\alpha^e_{nj} + \\
&+ \mu_k f^R_{kl}\left(\frac{\partial\mu_i}{\partial Q_a}\frac{\partial\alpha^e_{lj}}{\partial Q_a} + \frac{\partial\alpha^e_{li}}{\partial Q_a}\frac{\partial\mu_j}{\partial Q_a}\right)\frac{1}{\omega_a^2} + \left[\mu_k f^R_{kl}\alpha^e_{li}\frac{\partial\mu_m}{\partial Q_a}f^R_{mn}\frac{\partial\alpha^e_{nj}}{\partial Q_a} + \right. \\
&+ \left.\frac{\partial\alpha^e_{ki}}{\partial Q_a}f^R_{kl}\mu_l\frac{\partial\mu_m}{\partial Q_a}f^R_{mn}\alpha^e_{nj} + \frac{\partial\alpha^e_{ki}}{\partial Q_a}f^R_{kl}\mu_l\frac{\partial\alpha^e_{mj}}{\partial Q_a}f^R_{mn}\mu_n\right]\frac{1}{\omega_a^2}. \qquad (6.46)
\end{aligned}$$

By considering the fact that for molecules with certain symmetries vibrational modes are not simultaneous IR and Raman active, we have reason to believe that there are a number of terms in Eq. 6.42 that can be neglected which would further reduce the computational effort.

6.3.4 Effective properties and local field factors

A real experimental measurement is carried out with respect to the external field $F^{\rm E}$ which corresponds to the *effective properties*. Obviously, the connection to the *effective*

properties is different for *local field properties* and *cavity field properties* which means that different *local field factors* have to be used. For *local field properties* we have [55]

$$\alpha^{\text{eff}}_{ij}(-\omega;\omega) = l^{\omega}_{ia} f^{\text{C}\omega}_{ab}\ \alpha^{\text{L}}_{bj}(-\omega;\omega), \tag{6.47}$$

$$\beta^{\text{eff}}_{ijk}(-2\omega;\omega,\omega) = l^{2\omega}_{ia} l^{\omega}_{jb} f^{\text{C}\omega}_{bc} l^{\omega}_{kd} f^{\text{C}\omega}_{de}\ \beta^{\text{L}}_{ace}(-2\omega;\omega,\omega), \tag{6.48}$$

$$\begin{aligned}\gamma^{\text{eff}}_{ijkl}(-3\omega;\omega,\omega,\omega) = {} & l^{3\omega}_{ia} l^{\omega}_{jb} f^{\text{C}\omega}_{bc} l^{\omega}_{kd} f^{\text{C}\omega}_{de} l^{\omega}_{lf} f^{\text{C}\omega}_{fg}\ \gamma^{\text{L}}_{aceg}(-3\omega;\omega,\omega,\omega) \\ & + \left[\beta^{\text{L}}_{ica}(-3\omega;\omega,2\omega)\beta^{\text{C}}_{bde}(-2\omega;\omega,\omega)\right. \\ & + \beta^{\text{L}}_{ida}(-3\omega;\omega,2\omega)\beta^{\text{C}}_{bce}(-2\omega;\omega,\omega) \\ & \left. + \beta^{\text{L}}_{iea}(-3\omega;\omega,2\omega)\beta^{\text{C}}_{bcd}(-2\omega;\omega,\omega)\right] f^{\text{R}2\omega}_{ab} f^{\text{C}\omega}_{cj} f^{\text{C}\omega}_{dk} f^{\text{C}\omega}_{el},\end{aligned} \tag{6.49}$$

which shows that part of the effects from the induced reaction field have to be incorporated into the *local field factors*. For the *cavity field properties* we have

$$\alpha^{\text{eff}}_{ij}(-\omega;\omega) = f^{\text{C}\omega}_{aj}\ \alpha^{\text{C}}_{ia}(-\omega;\omega), \tag{6.50}$$

$$\beta^{\text{eff}}_{ijk}(-2\omega;\omega,\omega) = f^{\text{C}\omega}_{ja} f^{\text{C}\omega}_{kb}\ \beta^{\text{C}}_{iab}(-2\omega;\omega,\omega), \tag{6.51}$$

$$\gamma^{\text{eff}}_{ijkl}(-3\omega;\omega,\omega,\omega) = f^{\text{C}\omega}_{ja} f^{\text{C}\omega}_{kb} f^{\text{C}\omega}_{lc}\ \gamma^{\text{C}}_{iabc}(-3\omega;\omega,\omega,\omega). \tag{6.52}$$

which manifests that the whole effect of the total reaction field is accounted for in the properties rather than in the *local field factors*.

6.4 Examples of solvent effects on NLO properties

6.4.1 Saturation length of conjugated oligomers

It is well known that optical properties of conjugated oligomers in gas phase show a power-law dependence with respect to the length of the oligomer for a small number of units. For large N it becomes linear in N and the property per unit therefore becomes constant. This behavior has formed the base for different extrapolating procedures to obtain the values of optical properties of polymers [60]. Applying for instance the function used by Kirtman *et. al.* [61], i.e. a polynomial of order 9 in 1/N, one can estimate the length dependence of optical properties per unit for very long polyenes, i.e. polyacetylene, in solutions, as shown in Fig. 6.3.

The solvent environment makes the saturation (or correlation) length of both the polarizability and hyperpolarizability shorter. The saturation lengths of polyenes in strong polar solutions are found to be around N=22 and N= 60 for α_L and γ_L, respectively. It was pointed out by Champagne *et. al.* [62] from their calculations for short chain polyenes, that the local field factors tend toward unity with increasing chain length for the longitudinal component due to the fast decrease of κ_z. The simulations presented in this thesis certainly confirm their observations.

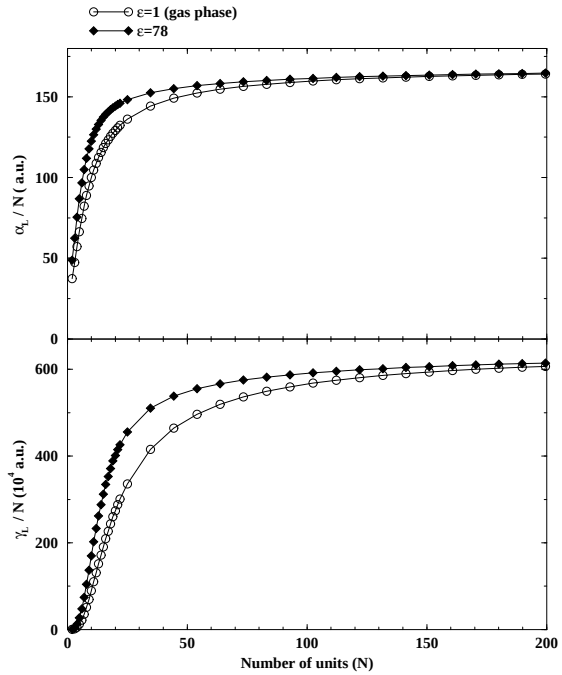

Figure 6.3: Length dependence of the (a) α_L/N, (b) γ_L/N for very long polyene chains in gas phase and polar solution.

6.4.2 Solvent effects on two-photon absorption

Recently, Kogej *et. al.* [63] studied structure-to-property relationships for TPA of donor-acceptor stilbene derivatives at the semi-empirical level. They showed that the TPA evaluation with respect to the bond-order alternation closely follows those of β. The TPA was found to be strongly dependent on the geometrical changes. It was concluded that such a behavior can be generalized to related conjugated compounds.

In Fig. 6.4, the solvent dependences of the TPA cross section of the first excited state and the static value of the first hyperpolarizability $\beta(0;0,0)$ are shown. The finite field approach with ellipsoidal cavity was employed in the calculation (paper V). The solvent dependence, as well as the geometrical dependence in terms of the bond length alternation (BLA) of β was found to be very large, more than twice the value in gas phase for the more polar solution. No saturation was reached. However, the saturation for the TPA cross section is different. The solvent dependence of TPA

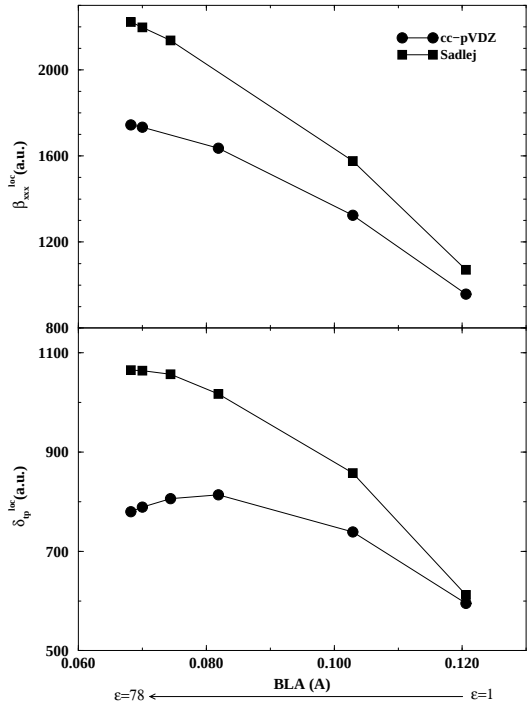

Figure 6.4: The solvent dependence of the static first hyperpolarizability $\beta(0;0,0)$ and the TPA cross section of the first excited state of NO_2–$(C_2H_2)_2$–NH_2 . The SCF/cc-pVDZ geometries are used.

is found to be smaller than that for β and it displays a saturation. Such a dependence indicate that the structure-to-property relationships for the TPA of donor-acceptor substitutes of stilbene can not be generalized to the case of push-pull polyenes.

Summary

In the present thesis I explored solvent and vibrational effects on nonlinear optical properties of organic molecules. *Ab initio* response theory calculations connected with dielectric continuum models were applied to large molecules.

The semiclassical model for solvent effects on nonlinear optical properties was generalized for ellipsoidal cavities including also vibrational contributions. *Ab initio* calculations of properties of isolated molecules together with the semiclassical model enabled a treatment of oligomers with a sufficient number of repeat units to study the solvent effects on their static polarizabilities and hyperpolarizabilities in the polymer limit. A solvent environment is shown to decrease the saturation lengths.

The existing ambiguity in the definition of the solute nonlinear optical properties with respect to the different perturbing fields was examined and connections between different conventions were presented. It was shown that special care must be taken when comparing theoretical and experimental solute properties. Proper local field factors for the nonlinear optical properties calculated by different dielectric continuum models were described. Using the comparison for the cases where the exact result is known the necessity of including the cavity field factor at the generated frequencies for the cavity based models was demonstrated.

Reaction field models were used to simulate macroscopic nonlinear optical properties observed in fullerene films. The semiclassical model and the self-consistent reaction field model were shown to be in agreement with experimental results. The calculations on fullerenes also showed the importance of using consistent local field factors.

Solvent effects on two-photon absorption were studied for push-pull molecules. In contrast to previous studies on stilbene derivatives, the solvent dependence of the two-photon absorption cross section of push-pull polyenes was found to be different than that of the first hyperpolarizability. The TPA cross section was found to be rather insensitive to the cavity choice.

The enhancement of the two-photon absorption in the multi-branched structures based on donor-π-acceptor chromophores was studied. The polarization dependence was found to be very important for the relative TPA cross sections. Numerical gradients of the two-photon absorption cross section were used to study the vibrational ef-

fects within the Herzberg-Teller approach. The vibrational contributions were shown to be the source for the unusually high TPA enhancement for certain classes of multi-branched molecules.

Apart from evaluating the vibrational contributions in the simple zero-order harmonic approximation for the excited state potential energy surface, displaced harmonic potential surfaces were considered. A method for calculating the TPA spectrum profile using a linear coupling model was derived and demonstrated. Sum rules were formulated for the vibrational contributions to TPA, showing that the overall integrated intensity gain due to vibrations is insensitive to the excited state potential surface and that it depends only on the gradient of the electronic TPA transition moment.

Structure-to-property relations were studied for the two-photon absorption in one dimensional donor/acceptor substituted $\pi-$conjugated molecules. The experimental findings that π-centers play a most crucial role in the design of two-photon absorption materials were confirmed. An electron-rich π-center attached to symmetrically substituted donors was found to constitute an optimal structure for maximizing the TPA cross sections in the visible region. Calculations indicated that while the one-photon absorption spectra of all molecules studied could be determined solely by the actual molecular length, this was clearly not possible for two-photon absorption. That indicates that it is not possible to obtain useful information about TPA activity from the one-photon absorption spectrum alone.

The large difference between the measured TPA cross section of molecules in solutions for short and long pulse durations was investigated. A dynamical model based on a density matrix formalism was developed. The non-resonant one-photon population of the lowest excited state with a following one-photon excited state absorption was identified as the main reason for the apparent enhancement of measured effective TPA cross sections for long pulses.

Acknowledgments

First of all, I would like to express my sincere gratitude to my supervisor Prof. Hans Ågren for introducing me to my research field and for creating a very stimulating and encouraging working environment with a constant flow of fresh ideas. I would also like to thank to my second supervisor Dr. Yi Luo for many discussions and the many suggestions he gave to me. The positive and optimistic attitude of my supervisors always helped me to solve problems arising during the course of my work.

I wish to thank Prof. Faris Gel'mukhanov for helping me to understand essential physics behind certain phenomena.

I would like to thank Dr. Patrick Norman, who helped me at the beginning of my work in the field of this thesis and for nice collaboration. I would also like to thank my other collaborators Prof. Robert W. Munn, Dr. Chuan-Kui Wang and Alexander Baev for nice and fruitful collaboration.

I would like to thank Prof. Trygve Helgaker for a nice and fruitful week spent in Oslo and for showing me how the gradients are implemented in the Dalton code. I also wish to thank Dr. Olav Vahtras for his hints and explanations of some parts of the response code.

It is very nice to be a part of the theoretical chemistry group. My thanks go to the present members Prof. Boris Minaev, Dr. Bernd Schimmelpfennig, Peter Cronstrand, Jin-Dong Guo, Stepan Kashtanov, Branislav Jansik, Oleksandr Loboda, Oscar Rubio-Pons, Lyudmyla Telyatnyk, Zilvinas Rinkevicius, Ingvar Tunell and Laban Pettersson as well as to the former members Dr. Olexandr Plashkevych, Dr. Timofei Privalov, Dr. Pawel Salek for the nice working atmosphere.

I would also like to express my thanks to Prof. Leif Johansson for giving me the opportunity to come to study in Sweden.

My brother Karol, and my parents always gave me invaluable support for me in all my work. Thank you.

And finally, my special thanks go to my wife Lubka for her love and support and of course to our little Martin, for all the joy he brought into our life.

Bibliography

[1] J.Kerr. *Phil. Mag.*, 50:337, 1875.

[2] P.A. Franken, A.E. Hill, C.W. Peters, and G. Weinreich. *Phys. Rev. Lett*, 7:118, 1961.

[3] M. Göppert-Mayer. *Ann. Phys. Lpz*, 9:273, 1931.

[4] W. Kaiser and C. G. Garret. *Phys. Rev. Lett*, 7:129, 1961.

[5] L.W. Tutt and T.F. Boggess. *Prog. Quantum. Electr.*, 17:299, 1993.

[6] S. Maruo, O. Nakamura, and S. Kawata. *Opt. Lett.*, 16:1780, 1991.

[7] H.-B. Sun, S. Matsuo, and H. Misawa. *Appl. Phys. Lett.*, 74:786, 99.

[8] J.D. Jackson. *Classical Electrodynamics*. 2nd Edn. Wiley, New York, 1975.

[9] Y.R. Shen. *The Principles of Nonlinear Optics*. John Wiley & Sons, New York, 1984.

[10] R.L. Sutherland. *Handbook of Nonlinear Optics*. Marcel Dekker, Inc., New York, 1996.

[11] M.G. Kuzyk and C.W. Dirk. *Characterization Techniques and Tabulations for Organic Nonlinear Optical Materials*. Marcel Dekker, Inc., New York, 1984.

[12] A.D.Buckingham. *J. Chem. Phys.*, 12:107, 1967.

[13] A. Willets, J.E. Rice, D.M. Burland, and D.P.Shelton. *J. Chem. Phys.*, 97:7590, 1992.

[14] H. Mahr. *Quantum Electronics*. H. Rabin and C.L. Tang, EDs.(Academic Press, New York), 1975.

[15] D.M. Bishop. *Rev. Mod. Phys.*, 62:343, 1990.

[16] C.J.F. Böttcher. *Theory of electric polarization, Vol. I*. Elsevier, Amsterdam, 1973.

[17] A. Szabo and N.S. Ostlund. *Modern Quantum Chemistry*. Macmillan, 1982.

[18] F. Jensen. *Introduction to Computational Chemistry*. John Wiley & Sons, 1999.

[19] T. Helgaker, P. Jørgensen, and J. Olssen. *Molecular Electronic-Structure Theory*. John Wiley & Sons, 2000.

[20] P. Hohenberg and W. Kohn. *Phys. Rev.*, 136:864, 1964.

[21] W. Kohn and L.J. Sham. *Phys. Rev. A*, 140:1133, 1965.

[22] J. Olsen and P. Jørgensen. *J. Chem. Phys.*, 82:3235, 1985.

[23] H.J.Aa. Jensen and H. Ågren. *Chem. Phys.*, 104:229, 1986.

[24] O. Christiansen, P. Jørgensen, and C. Hättig. *Int. J. Quant. Chem.*, 68:1, 1998.

[25] D. Bishop and B. Kirtman. *J. Chem. Phys.*, 95:2646, 1991.

[26] T.U. Helgaker and J. Almlöf. *J. Chem. Phys.*, 84:6266, 1986.

[27] J. Oddershede. *Adv. Chem. Phys.*, 69:201, 1987.

[28] E.S. Nielsen, P. Jørgensen, and J. Oddershede. *J. Chem. Phys.*, 73:6238, 1980.

[29] B.A. Reinhardt. *Phot. Sci. News*, 4:21, 1998.

[30] B.A. Reinhardt, L.L. Bott, S.J. Clarson, A.G. Dillard, J.C. Bhatt, R. Kannan, L. Yuan, G.S. He, and P.N. Prasad. *Chem. Mater.*, 10:1863, 1998.

[31] O.-K. Kim, K.-S. Lee, H.Y. Woo, K.-S. Kim, G.S. He, J. Swiatkiewicz, and P.N. Prasad. *Chem. Mater.*, 12:284, 2000.

[32] P. R. Monson and W. M. McClain. *J. Chem. Phys.*, 53:29, 1970.

[33] M. Albota, D. Beljonne J. L. Brédas, J. E. Ehrlich, J. Fu, A. A. Heikal, S. E. Hess, T. Kogej M. D. Levin, S. R. Marder, D. McCord-Maughon, J. W. Perry, H. Röckel, M. Rumi, G. Subramaniam, W. W. Webb, X. Wu, and C. Xu. *Science*, 281:1653, 1998.

[34] K.D. Belfield, D.J. Hagan, E.W. van Stryland, K.J. Schafer, and R.A. Negres. *Org. Lett*, 1:1575, 1999.

[35] L. Ventelon, L. Moreaux, J. Mertz, and M. Blanchard-Desce. *Chem. Commun.*, 20:2055, 1999.

[36] M. Albota *et. al. Science*, 281:1653, 1998.

[37] P. Norman, Y. Luo, and H. Ågren. *J. Chem. Phys.*, 111:7758, 1999.

[38] S. J. Chung, K. S. Kim, T. C. Lin, G. S. He, J. Swiatkiewitz, and P. N. Prasad. *J. Phys. Chem. B*, 103:10741, 1999.

[39] G.S. He, L. Yuan, N. Cheng, J.D. Bhawalkar, P.N. Prasad, L.L. Brott, S.J. Clarson, and B.A. Reinhardt. *J. Opt. Soc. Am. B*, 14:1079, 1997.

[40] J. Swiatkiewicz, P.N. Prasad, and B.A. Reinhardt. *Opt. Commu.*, 157:135, 1998.

[41] M. Born. *Z. Phys.*, 1:45, 1920.

[42] J.G. Kirkwood. *J. Chem. Phys.*, 2:351, 1934.

[43] L.Onsager. *J. Am. Chem. Soc.*, 58:1486, 1936.

[44] J.A.Stratton. *Electromagnetic Theory*. McGraw-Hill, New York, 1941.

[45] K. V. Mikkelsen, H. Ågren, H. J. Aa. Jensen, and T. Helgaker. *J. Chem. Phys.*, 89:3086, 1988.

[46] K. V. Mikkelsen, P. Jørgensen, and H. J. Aa. Jensen. *J. Chem. Phys.*, 100:6597, 1994.

[47] K. V. Mikkelsen and K. O. Sylvester-Hvid. *J. Phys. Chem.*, 109:9116, 1996.

[48] S. Miertus, E. Scrocco, and E. Tomasi. *J. Chem. Phys.*, 55:117, 1981.

[49] S. Miertus and E. Tomasi. *J. Chem. Phys.*, 65:239, 1982.

[50] J.L. Pascual-Ahuir, E. Sila, J. Tomasi, and R.J. Bonaccorsi. *J. Comput. Chem.*, 8:778, 1987.

[51] M.A. Aguilar, F.J. Olivares del Valle, and J. Tomasi. *J. Chem. Phys.*, 98:778, 1993.

[52] J. Tomasi and M. Persico. *Chem. Rev.*, 94:2027, 1994.

[53] R. Cammi, B. Mennucci, and J. Tomasi. *J. Phys. Chem. A*, 102:870, 1997.

[54] Y. Luo, P. Norman, and H. Ågren. *J. Chem. Phys.*, 109:3589, 1998.

[55] P. Macak, P. Norman, Y. Luo, and H. Ågren. *J. Chem. Phys.*, 112:1868, 2000.

[56] R. Wortmann and D. M. Bishop. *J. Chem. Phys.*, 108:1001, 1998.

[57] P. Norman, P. Macak, Y. Luo, and H. Ågren. *J. Chem. Phys.*, 110:7960, 1999.

[58] A. Willetts and J.E. Rice. *J. Chem. Phys.*, 99:426, 1993.

[59] P. Norman, Y. Luo, and H. Ågren. *J. Chem. Phys.*, 109:3580, 1998.

[60] E.K. Dalskov, J. Oddershede, and D.M. Bishop. *J. Chem. Phys.*, 108:1001, 1998.

[61] B. Kirtman, J. Toto, K. Robins, and M. Hasan. *J. Chem. Phys.*, 102:5350, 1995.

[62] B. Champagne, B. Mennucci, M. Cossi, R. Cammi, and J. Tomasi. *J. Chem. Phys.*, 238:153, 1998.

[63] T. Kogej, D. Beljonne, F. Meyers, J. W. Perry, S. R. Marder, and J. L. Brédas. *Chem. Phys. Lett.*, 298:1, 1998.